*Cerebral Cortex*, 2018; 1–21

**doi: 10.1093/cercor/bhy096**
Original Article

ORIGINAL ARTICLE

# Hippocampal Radial Glial Subtypes and Their Neurogenic Potential in Human Fetuses and Healthy and Alzheimer's Disease Adults

Sara Cipriani[1], Isidre Ferrer[2], Eleonora Aronica[3], Gabor G. Kovacs[4], Catherine Verney[1], Jeannette Nardelli[1], Suonavy Khung[5], Anne-Lise Delezoide[5], Ivan Milenkovic[4], Sowmyalakshmi Rasika[1], Philippe Manivet[6], Jean-Louis Benifla[7], Nicolas Deriot[6,8], Pierre Gressens[1,9] and Homa Adle-Biassette[1,6,8]

[1]PROTECT, INSERM, Université Paris Diderot, Sorbonne Paris Cité, F-75019 Paris, France, [2]Department of Pathology and Experimental Therapeutics, University of Barcelona, Bellvitge Campus, L'Hospitalet de Llobregat, Spain; Centre for Networked Biomedical Research in Neurodegenerative Diseases (CIBERNED), Institute Carlos III, Madrid, Spain, [3]Department of (Neuro)Pathology, Academic Medical Center, University of Amsterdam, Meibergdreef 9, 1105 AZ Amsterdam, The Netherlands, [4]Institute of Neurology, Medical University of Vienna, Vienna, Austria, [5]APHP, Service de Biologie du Développement, Hôpital Robert-Debré, APHP, Paris, France, [6]APHP, Plateforme de Bio-Pathologie et de Technologies Innovantes en Santé, Centre de Ressources Biologiques BB-0033-00064, Hôpital Lariboisière, Paris, France, [7]APHP, Service de Gynécologie-Obstétrique, Hôpital Lariboisère, 75010 Paris, France, [8]Service d'Anatomie et de Cytologie Pathologiques, Hôpital Lariboisère, 75010 Paris, France and [9]Department of Division of Imaging Sciences and Biomedical Engineering, Centre for the Developing Brain, King's College London, King's Health Partners, St. Thomas' Hospital, London, SE1 7EH, UK

Address correspondence to Homa Adle-Biassette, Department of Pathology, Lariboisière Hospital, 2 Rue Ambroise Paré, 75010 Paris, France. Email: homa.adle@inserm.fr.

## Abstract

Neuropathological conditions might affect adult granulogenesis in the adult human dentate gyrus. However, radial glial cells (RGCs) have not been well characterized during human development and aging. We have previously described progenitor and neuronal layer establishment in the hippocampal pyramidal layer and dentate gyrus from embryonic life until mid-gestation. Here, we describe RGC subtypes in the hippocampus from 13 gestational weeks (GW) to mid-gestation and characterize their evolution and the dynamics of neurogenesis from mid-gestation to adulthood in normal and Alzheimer's disease (AD) subjects. In the pyramidal ventricular zone (VZ), RGC density declined with neurogenesis from mid-gestation until the perinatal period. In the dentate area, morphologic and antigenic differences among RGCs were observed from early ages of development to adulthood. Density and proliferative capacity of dentate RGCs as well as neurogenesis were strongly reduced during childhood until 5 years, few $DCX^+$ cells are seen in adults. The dentate gyrus of both control and AD individuals showed $Nestin^+$ and/or $GFAP\delta^+$ cells displaying different morphologies. In conclusion, pools

of morphologically, antigenically, and topographically diverse neural progenitor cells are present in the human hippocampus from early developmental stages until adulthood, including in AD patients, while their neurogenic potential seems negligible in the adult.

**Key words:** adult neurogenesis, hippocampus, human fetal brain, neurogenesis, radial glial cells

## Introduction

The seminal study by Eriksson et al. (1998) provided direct evidence for adult neurogenesis in the human hippocampal dentate gyrus. Adult hippocampal neurogenesis in rodents can be modulated by physical activity, dietary restriction, environmental enrichment, and various kinds of injury including epilepsy and stroke (Kempermann et al. 1997, 2002; van Praag, Christie, et al. 1999; van Praag, Kempermann, et al. 1999; Scott et al. 2000; Lee et al. 2002; Brown et al. 2003; Monje 2003; Darsalia et al. 2005; Smith et al. 2006). Deficits in granular neurogenesis are thought to be involved in the etiology of memory impairment, and neuropsychiatric and neurodegenerative diseases in rodents (Feng et al. 2001; Wen et al. 2004; Winocur et al. 2006; Denis-Donini et al. 2008; Ibi et al. 2008; Ma et al. 2008; Li et al. 2010) and in humans (Reif et al. 2006; Boldrini et al. 2009; Lucassen et al. 2010). It has been suggested that adult hippocampal neurogenesis may thus represent a new pharmacological target in such conditions. However, few studies to characterize neural progenitor cells (NPC) in the human dentate gyrus have been performed so far.

A reduction in the number of Nestin-positive cells and β-III-tubulin-expressing cells has been observed, post-mortem, in the dentate subgranular zone (SGZ) of individuals with Parkinson's disease ($n = 8$) as compared with controls ($n = 3$) (Höglinger et al. 2004). Jin et al. (2004) reported increases in the amount of proneurogenic proteins in Alzheimer's disease (AD) tissues detected by Western blot and immunohistochemical analyses. Boekhoorn et al. (2006) showed an increase in hippocampal proliferation in presenile AD patients, mainly observed in CA1-3, but related to a gliotic and vascular response rather than to neurogenesis; they also showed the presence of artifactual granular doublecortin (DCX) immunoreactivity. Reif et al. (2006) reported a reduction in the number of $Ki67^+$ cells in the dentate gyrus of individuals with schizophrenia but not with depression, However, five subjects (healthy controls as well as schizophrenic and depressive subjects) who displayed dramatically increased levels of proliferation in the dentate gyrus were excluded from the study and the phenotype of their proliferative cells was not studied. Boldrini et al. (2009) found a reduction in proliferation in non-treated depressed individuals whereas antidepressant-treated patients had higher numbers in the rostral DG. Lucassen et al. (2010) reported a reduced number of $MCM2^+$ cells in the granule cell layer (GCL) and SGZ of depressed patients, without a stimulatory effect of antidepressants on dentate cell proliferation.

Therefore, little information about human adult neurogenesis and neural stem/progenitor cells exists to justify the investment of resources in developing new treatments in humans, and most of the available evidence is inconclusive or contradictory. These discrepancies may be due to the insufficient number of cases and controls, the inclusion and exclusion criteria, the choice of antibodies or the methods used for the detection and quantification of proliferating cells. Moreover, in general, the subtype and/or the fate of proliferating cells were not studied. In some studies, the immunolabeling was obviously non-specific, such as the expression of cytoplasmic markers in the nucleus (or vice versa) or autofluorescence due to lipofuscin interpreted as a positive immunolabeling signal (Adle-Biassette et al. 2007).

To date, it is not clear to what extent adult neurogenesis shares common features with developmental neurogenesis, and whether dentate NPCs persist in individuals with AD. Several putative markers of adult stem cells have been described in humans and mice (Morshead et al. 1994; Mignone et al. 2004; Encinas et al. 2011; Dranovsky et al. 2012). Nestin expression has been reported in the hippocampus of adult humans (Crespel et al. 2005). Nestin is an intermediate filament, expressed by quiescent and proliferating neural stem/progenitors cells (Lendahl et al. 1990; Morshead et al. 1994; Dahlstrand et al. 1995; Michalczyk and Ziman 2005). In humans, the expression of GFAPδ has been reported in the subventricular zone (SVZ) of the lateral ventricle (Roelofs et al. 2005; van den Berge et al. 2010), the dentate gyrus (Roelofs et al. 2005), and the olfactory bulb (van den Berge et al. 2010). GFAPδ is an isoform of glial fibrillary acidic protein (GFAP), a type III intermediate filament protein (Fuchs 1998), which interacts with the γ-secretase complex, a crucial mediator of Notch signaling (Nielsen et al. 2002), and is likely important for NPC self-renewal. Moreover, GFAPδ is also expressed in fetal NPCs of the mouse hippocampus and human neocortex (Middeldorp et al. 2010; Mamber et al. 2012). PAX6 and vimentin, which are both markers of RGCs/neural stem cells (Levitt et al. 1981; Götz et al. 1998; Kamei et al. 1998; Zecevic et al. 1999; Quinn et al. 2007), are also involved in hippocampal neurogenesis (Hevner et al. 2006; Lavado et al. 2010; Cipriani et al. 2016, 2017). In comparison, the neuronal progenitor marker Tbr2 is required for neuronal lineage progression to granule cells in newborn mice (Hodge et al. 2012, 2013; Berg et al. 2015), and the microtubule-associated protein DCX is expressed by immature neurons (Francis et al. 1999; Gleeson et al. 1999).

We have previously used several of these markers to characterize proliferating NPCs in the pyramidal layer of the hippocampal formation (Ammon's horn) and in various germinal matrices of the dentate gyrus from 9 GW until mid-gestation in human fetuses (Cipriani et al. 2016, 2017; Supplementary Fig. 7). These studies showed that the mechanisms of neurogenesis in the developing dentate gyrus are different from those observed in the pyramidal layer of the hippocampal formation. The latter mimic to some extent those observed in the neocortex (Leid et al. 2004; Nieto et al. 2004; Britanova et al. 2005; Englund 2005; Szemes et al. 2006; Bayatti et al. 2008; Bedogni et al. 2010; Han et al. 2011), although major regional differences such as neuronal subtypes and lamination exist (Cipriani et al. 2016, 2017). At GW 13, the Ammon's horn includes two germinal compartments, the ventricular zone (VZ) containing $PAX6^+$ cells and the SVZ containing $PAX6^+$ and $TBR2^+$ cells (Cipriani et al. 2016) and an intermediate zone (IZ) corresponding to the entire area between the SVZ and the pyramidal plate, as in the neocortex (Bystron et al. 2008). In the dentate area (Cipriani et al. 2017), the secondary matrix (ds) composed of proliferative $PAX6^+$ and

TBR2$^+$ progenitors surrounds the dentate anlage streaming toward the subpial layer and to some extent, into the cluster of the dentate anlage where post-mitotic granule neurons are present. By GW 16, the hippocampal formation had gyrated, the hippocampal fissure had started to close and the GCL could be delineated and surrounded a hilar matrix containing PAX6$^+$ cells and some TBR2$^+$ progenitors. The main germinal areas include the subpial stream of the secondary dentate matrix extending toward the developing internal limb and into the hilus.

The aim of the present study was to extend our previous findings by investigating neural stem/progenitor cells and the dynamics of their neurogenic potential in the human hippocampal formation from fetal life to adulthood. We focused on the transition between developmental (from gestational week, GW 13) and adult dentate neurogenesis. Neural stem/progenitor cells have been identified by immunolabeling with antibodies against GFAPδ and other progenitor cell markers, such as Nestin, vimentin, SOX2, PAX6, TBR2, and their proliferation has been analyzed by immunodetection of both Ki67 (Gerdes et al. 1991) and MCM2 markers, as previously reported (Lucassen et al. 2010; Liu et al. 2018). Furthermore, we assessed the hippocampal formation of individuals with AD for abnormalities in the expression of stem cell and cell fate markers.

## Materials and Methods

### Samples

The cases included in this study were selected from the brain banks of INSERM Unit 1141, Paris, France; the Department of Neuropathology of the Academic Medical Center, University of Amsterdam, The Netherlands; the Institute of Neuropathology HUB-ICO-IDIBELL Biobank, Barcelona, Spain, and the Institute of Neurology, Medical University of Vienna, Austria (Tables 1 and 2). Informed consent was obtained for the use of brain tissue and for access to medical records for research purposes.

Ten fetuses were collected after spontaneous death or legal abortion, with written maternal consent. The gestational age of each case was estimated on the basis of anatomy and pregnancy records. Hippocampal tissues from 10 infants and 19 adult donors (average age: 50 years), whose cause of death was not related to genetic disorders, head injury, or neurological diseases, and from five cases with AD (stage V–VI) (average age: 81 years) were also studied. Neuropathological diagnosis of AD was carried out according to Braak stages (Braak and Braak 1991, 1995) adapted to paraffin sections (Braak et al. 2006). All procedures followed European Union legislation and were approved by the local ethics committees.

### Histology

For frozen sections, tissue was fixed in 4% paraformaldehyde, cryoprotected in 20% sucrose and stored at −80 °C until use. Samples were cut into 12-µm thick cryosections, mounted on Superfrost slides and stored at −80 °C. For paraffin sections, samples were embedded in paraffin and cut into 5-µm thick sections. Antigen retrieval was performed in citrate buffer for 1 h at 94 °C (1.8 mM citric acid, 8.2 mM sodium citrate, pH 6) before immunolabeling. For MCM2 immunofluorescence immunostaining, antigen retrieval was performed in citrate buffer for 30 min at 94 °C. Frozen and paraffin sections were permeabilized with 0.1% Triton X-100 dissolved in 0.12 M phosphate buffer (pH 7.4). Sections were loaded with primary antibodies for ~16 h at 4 °C according to the concentrations reported in Table 3. Labeling was revealed by Alexa Fluor 488-, Alexa Fluor 555-, or Alexa Fluor 676-conjugated secondary antibodies (1:500, Invitrogen Molecular Probes).

In order to perform double-labeling using same-source antibodies, we employed the Tyramide Signal Amplification (TSA) System (PerkinElmer). Briefly, the first primary antibody was revealed with TSA-cy3 as described by the manufacturer. Then, sections were treated at 94 °C with buffer citrate (1.8 mM acid citric, 8.2 mM sodium citrate, pHn6) for 15′. After three washes in PBS, the second primary antibody was loaded and revealed as described above.

Nuclei were labeled using 4′,6-diamidino-2-phenylindole (DAPI, 1 µg/ml, Invitrogen Molecular Probes), and coverslips mounted with Fluoromount-G mounting medium (SouthernBiotech, Birmingham, USA). Tissue from adult donors was treated with a saturated solution of Sudan Black B (30′ at 25 °C) before coverslipping, in order to remove autofluorescence due to lipofuscin.

Paraffin embedded sections were immunolabeled for Ki67 (1/50, CC1:90 min), Sox2, Nestin and DCX using the BenchMark ULTRA automated staining system.

**Table 1.** Control cases

| Cases | Age | Tissue processing | Post-mortem delay/fixation time |
|---|---|---|---|
| 1 | GW 13 | Frozen | NA |
| 2 | GW 16 | Paraffin | NA |
| 3 | GW 18 | Paraffin | NA |
| 4 | GW 19 | Frozen | 24 h/72 h |
| 5 | GW 22 | Frozen | 8 h/24 h |
| 6 | GW 25 | Frozen | NA |
| 7 | GW 30 | Frozen | NA |
| 8 | GW 30 | Paraffin | NA |
| 9 | GW 38 | Frozen/paraffin | NA |
| 10 | GW 39 | Frozen | NA |
| 11 | 17 Days | Paraffin | 24 h/72 h |
| 12 | 22 Days | Paraffin | 10 h/10 h |
| 13 | 2 months | Paraffin | 8 h/24 h |
| 14 | 2.5 months | Paraffin | NA |
| 15 | 4 Months | Paraffin | NA |
| 16 | 5 Months | Paraffin | NA |
| 17 | 2 Years | Paraffin | NA |
| 18 | 5 Years | Paraffin | NA |
| 19 | 7 Years | Paraffin | NA |
| 20 | 10 Years | Paraffin | NA |
| 21 | 23 Years | Paraffin | NA |
| 22 | 29 Years | Paraffin | NA |
| 23 | 35 Years | Paraffin | NA |
| 24 | 41 Years | Paraffin | 12 h |
| 25 | 42 Years | Paraffin | NA |
| 26 | 45 Years | Paraffin | 20 h |
| 27 | 45 Years | Paraffin | 4 h |
| 28 | 47 Years | Paraffin | 10 h |
| 29 | 51 Years | Paraffin | 4 h |
| 30 | 52 Years | Paraffin | NA |
| 31 | 54 Years | Paraffin | 8 h |
| 32 | 54 Years | Paraffin | 9 h |
| 33 | 57 Years | Paraffin | NA |
| 34 | 59 Years | Paraffin | NA |
| 35 | 60 Years | Paraffin | NA |
| 36 | 61 Years | Paraffin | NA |
| 37 | 63 Years | Paraffin | NA |
| 38 | 65 Years | Paraffin | NA |
| 39 | 72 Years | Paraffin | NA |

**Table 2.** Alzheimer's disease cases

| Cases | Age (years) | Tissue processing | Post-mortem delay/ fixation time | Diagnosis (Braak stages) |
|---|---|---|---|---|
| 1 | 74 | Paraffin | 9 h | AD V–VI |
| 2 | 78 | Paraffin | 17 h | AD V–VI |
| 3 | 79 | Paraffin | 4 h | AD V–VI |
| 4 | 86 | Paraffin | 23 h | AD V–VI |
| 5 | 89 | Paraffin | 3 h | AD V–VI |

### Microscopy

Tile scans were acquired by means of a Zeiss Axio Observer.Z1 fluorescent microscope with the following excitation/emission beams: 359/461 nm for DAPI, 470/509 nm for Alexa Fluor 488, 558/583 nm for Alexa Fluor 555 and 649/670 nm for Alexa Fluor 647, using a Plan-Apochromat 20×/0.8 M27 objective and AxioCamMR3 camera. Images were then processed using Axiovision Rel. 4.8 software (Zeiss) and contrast adjusted with Adobe Photoshop CS3 (Adobe Systems, Mountain View, CA, USA).

Confocal analysis was performed with a Leica TCS SP8 confocal scanning system (Leica Microsystems) equipped with a 405 nm Diode, 488 nm Ar, 561 nm DPSS and 633 nm HeNe lasers. Eight-bit digital images were collected from a single optical plane using a 20× HC PL APO CS2 oil-immersion objective (numerical aperture 0.75; Leica) or a 40× HC PL APO CS2 oil-immersion objective (numerical aperture 1.30; Leica). For each sample, optical sections of 2048 × 2048 pixels were imaged at 0.9 µm intervals. Images were processed with LAS AF.Ink software (Leica). Z-stack images were then analyzed with ImageJ software (National Institutes of Health, USA). Images were assembled into photomontages using QuarkXPress (Quark Inc., Denver, CA, USA).

## Results (High-resolution enlargeable images are available on the website)

For a summary of the main developmental steps see Supplementary Fig. 7, and for a summary of the results see Table 4.

### GW 13

We have previously described the evolution and serial appearance of germinal compartments during fetal hippocampal neurogenesis, including the presence of two germinal compartments in Ammon's horn and the formation of the secondary dentate matrix (Cipriani et al. 2016, 2017). In the present study, to assess the morphological and antigenic features of fetal hippocampal progenitor cells, we performed double-labeling for the progenitor markers GFAPδ and vimentin, Nestin, PAX6, TBR2, as previously described (Cipriani et al. 2016, 2017).

In the VZ of Ammon's horn and fimbria, Nestin$^+$ (Fig. 1*A*), vimentin$^+$ (Fig. 1*B*,*K*), and PAX6$^+$ (Fig. 1*C*,*L*) apical radial glial cells (RGCs) and their processes were radially oriented towards the Ammonic plate and the subpial layer, respectively. GFAPδ immunolabeling was observed both in the somata and processes of RGCs (Fig. 1*B–D*, *K–M*) where it overlapped with the pattern of vimentin. Some RGCs of the SVZ and IZ displayed no apical contacts, resembling basal RGCs of the neocortex (Fig. 1*B–D*). About 25% of PAX6$^+$ and 41% of GFAPδ$^+$ cells co-expressed Ki67.

In the dentate VZ (dVZ), Nestin$^+$ cells lacked the characteristic radial organization and displayed multiple processes (Fig. 1*A*). Nestin$^+$ cells were also labeled for GFAPδ, vimentin, and PAX6 (Fig. 1*E–G*). In the secondary dentate matrix, Nestin$^+$ (Fig. 1*A*), and GFAPδ$^+$/vimentin$^+$ cells were tangentially oriented around the dentate anlage, bearing unipolar or bipolar fibers (Fig. 1*H–J*). GFAPδ labeled ~95% of cells, one-third of which were proliferating progenitors (Fig. 1*J*). In contrast, within the cluster of cells forming the dentate anlage, GFAPδ$^+$/vimentin$^+$ progenitors with unipolar or bipolar processes were less abundant (Fig. 1*H–J*). GFAPδ labeled ~8% of cells, 38% of which were proliferating progenitors (Fig. 1*J*).

In the Ammonic, dentate and fimbrial areas, GFAPδ labeling completely overlapped with vimentin (Fig. 1*B*,*E*,*H*,*K*), but only partially (~70%) with PAX6 expression (Fig. 1*C*,*F*,*I*,*L*). Ki67 labeling was observed in both GFAPδ$^+$/PAX6$^+$ and GFAPδ$^+$/PAX6$^-$ cells (Fig. 1*D*,*G*,*J*), suggesting that GFAPδ labeled different progenitor cell populations.

In summary, these data suggest the presence of distinct types of glial progenitor cells in the Ammonic VZ, fimbria, dentate matrix, and anlage, based on their differential expression of Nestin, vimentin, GFAPδ, and PAX6. At this stage, the external shell of the dentate anlage starts to form from the secondary dentate matrix, while the hilus is not yet well organized.

### GW 16–22

A previous study has shown that at GW 16, the hippocampal formation has rotated and the hippocampal fissure has started to close (Humphrey 1967). In the dentate gyrus, the GCL, and the hilus are identifiable. From GW 16 to 20, the Ammonic VZ is reduced in thickness and proliferative capacity (Cipriani et al. 2016). Conversely, the subpial secondary dentate matrix and the hilar matrix, containing PAX6$^+$ and TBR2$^+$ progenitor cells, are highly proliferative (Cipriani et al. 2017).

In the present study, in the Ammonic VZ, Nestin, vimentin, GFAPδ, and PAX6 still labeled apical- and basal-like RGCs in the VZ and SVZ/IZ (Fig. 2*A–F*, Supplementary Figs 1.*A–D* and 2*D*). Around 5% of PAX6$^+$ cells were colabeled with Ki67 at GW 20. GFAPδ was observed in vimentin$^+$ (Fig. 2*D*), Nestin$^+$ (Fig. 2*E*), and PAX6$^+$ cells (Fig. 2*F*, Supplementary Fig. 1D). Due to the rotation of the hippocampus, several RGC processes were tangentially oriented toward the pyramidal layer, especially in the prospective CA1 (Fig. 2*D–F*), as compared with CA2-3 (Supplementary Figs 1D and 2*A–D*).

In the dentate area, Nestin and vimentin labeling increased between GW 16 and 22. The SGZ became identifiable as a dense band of Nestin$^+$ cells underlying the granule layer (Fig. 2*A*,*H*; Supplementary Figs 1A, 2*A*,*B*,*E*, and 4*A*). In the hilus and SGZ, numerous RGCs had unipolar radial processes oriented toward the GCL and branching upon entering the molecular layer (Fig. 2*G*,*H*; Supplementary Figs 2*A*,*B*,*E* and 4*A*). GFAPδ labeling was detected in several vimentin$^+$ (Fig. 2*G*), Nestin$^+$ (Fig. 2*H*) and PAX6$^+$ cells (Fig. 2*I*) of the hilus. However, the secondary dentate matrix was more intensely labeled with GFAPδ (Fig. 2*B*, Supplementary Fig. 1*B*,*F*) and showed a partial overlapping of expression between GFAPδ and vimentin (~70%) (Fig. 2*J*), Nestin (~50%) (Fig. 2*K*) and PAX6$^+$ (~70%) (Fig. 2*L*, Supplementary Fig. 1*E*,*F*). Some of these were proliferating progenitor cells, as shown by colabeling for GFAPδ/Ki67 (around 7% of GFAPδ$^+$ cells were colabeled with Ki67) (Supplementary Fig. 1*G*, *I*), PAX6/Ki67 (~10% of PAX6$^+$ cells were colabeled with Ki67) and vimentin/Ki67 (~5% of Vimentin$^+$ cells were colabeled with Ki67) (Supplementary Fig. 2*E*,*F*), and confirmed by colabeling for Nestin and the alternative proliferation marker MCM2, which

**Table 3.** Antibodies employed in the study

| Antibody | Company | Species | Concentration used on frozen/paraffin sections | Target |
|---|---|---|---|---|
| Proliferation | | | | |
| Ki67 | Abcam, ab27619 | Rabbit | 1:200/- | Cell cycle related nuclear protein |
| Ki67 | Dako, M7240 (Clone MIB) | Mouse | 1:500/1:50 | Cell cycle related nuclear protein |
| MCM2 | Santa Cruz sc-9839 | Goat | 1:100 | |
| Neuronal progenitors | | | | |
| SOX2 | Abcam, ab97959 | Rabbit | 1:200/1:100 | Stem cell self-renewal transcription factor |
| PAX6 | Proteintech, 12323-1-AP | Rabbit | 1:200/1:100/1:2,000 | Stem cell transcription factor |
| PAX6 | DSHB | Mouse | 1:10/- | Stem cell transcription factor |
| TBR2 | Abcam, ab23345 | Rabbit | 1:200-/1:3,000 | Transcription factor present in neurogenic intermediate progenitors |
| GFAPδ | Millipore AB9598 | Rabbit | 1:2,000/1:1,000/1:3,000 | Class-III intermediate filament |
| Vimentin | Leica, VIM-572-L-CE | Mouse | 1:500/1:50/1:3,000 | Intermediate filament protein |
| Nestin | Millipore ABD69 | Rabbit | 1:500/1:200 | Intermediate filament protein |
| Nestin | Millipore MAB5326 | Mouse | 1:500/1:200 | Intermediate filament protein |
| Post-mitotic cells | | | | |
| Doublecortin | Abcam Ab18723 | Rabbit | 1:4,000/1:2,000 | Microtubule-associated protein in immature neurons |
| Doublecortin | Millipore AB2253 | GuineaPig | 1:4,000/1:2,000 | Microtubule-associated protein in immature neurons |
| Tuj1 | Eurogentec MMS-435P | Mouse | 1:4,000/1:2,000 | The major microtubule protein |

**Table 4.** Summary of the results

| | Ammon's horn | Dentate gyrus |
|---|---|---|
| GW 13 | Apical and monopolar RGCs in the VZ/SVZ are labeled for PAX6 (of which 25% are Ki67$^+$), nestin, vimentin, and GFAPδ (of which 41% are Ki67$^+$). | Monopolar and bipolar RGCs in the secondary dentate matrix surround the dentate anlage, labeled for PAX6, nestin, vimentin, and GFAPδ (of which 30% are Ki67$^+$). Progenitors are less abundant in the dentate anlage (8% of dentate cells are GFAPδ$^+$, of which 38% are Ki67$^+$). |
| GW 16 –22 | RGCs are still labeled for PAX6 (of which 5% are Ki67$^+$ at GW 20) nestin, vimentin, and GFAPδ. | The GCL, the SGZ and the hilus are identifiable. Progenitors increase in density. In the SGZ/hilus, numerous RGCs bearing unipolar radial processes are oriented toward the GCL and labeled with PAX6 (of which 10% are Ki67$^+$), nestin, vimentin, and GFAPδ (7% of which are Ki67$^+$). |
| GW 25–30 | Numerous SOX2$^+$ and PAX6$^+$ cells are still observed in the VZ, without detectable colabeling with Ki67. Numerous DCX$^+$ cells are present in the SVZ and superficial pyramidal layer. | Progenitors are still dense in the SGZ/hilus (50% of the cells are nestin$^+$ and 30% PAX6$^+$, of which 7% are Ki67$^+$ cells). GFAPδ$^+$ cells are observed at the FDJ. |
| GW 38—5 Months | Several GFAPδ$^+$/PAX6$^+$ cells are observed in the ependymal layer. | Progenitors are still dense in the SGZ/hilus (30% of the cells are nestin$^+$ and PAX6$^+$) and proliferate predominantly near the internal limb of the DG (12% of nestin$^+$ cells coexpress Ki67$^+$ and 2% of PAX6$^+$ cells coexpress Ki67), but their density and proliferation decline after birth. |
| | Numerous DCX$^+$ cells are observed in the SVZ and pyramidal layer. | Numerous newly generated DCX$^+$ and TUJ1$^+$ neurons are present (30% of the SGZ cells). |
| 2–10 Years | Some Nestin and/or GFAPδ$^+$/Ki67$^-$ cells are detectable in the SVZ. | 6% of SGZ/hilar cells express nestin, of which 13% are Ki67$^+$ at 2 years. |
| | There are no DCX-expressing cells. | DCX$^+$/TUJ1$^+$ cells represent 5% of granule cells at 2 years, and their density decreases until 5 years. |
| Adults | Ribbon of Nestin$^+$ and/or GFAPδ$^+$ cells is seen in the SVZ. | There are very few RGC-like nestin$^+$ cells. |
| | There are no DCX-expressing cells. | A few DCX$^+$ cells are present (>1% of granule cells). |

allowed more cycling NPCs to be detected than Ki67 (around 30%) (not shown). Few GFAPδ$^+$ or Nestin$^+$ cells were colabeled for TBR2 (Supplementary Fig. 1*H*), suggesting that GFAPδ expression predominated in RGCs.

In the fimbria, GFAPδ labeling was detected in vimentin$^+$, Nestin$^+$, and PAX6$^+$ RGCs of the VZ and upper VZ (a more appropriate term than SVZ in the fimbria) (Fig. 2*M–O*, Supplementary Fig. 1*J*). Some proliferating Ki67$^+$/GFAPδ$^+$ cells (~2% of GFAPδ$^+$ cells) were found in the upper VZ (Supplementary Fig. 1*K*).

In summary, vimentin, Nestin, and GFAPδ labeled several subtypes of RGCs, presumably with different neurogenic potentials, in the Ammonic VZ, SVZ, dentate area, and fimbria. The SGZ and the hilus of the dentate anlage had at least partly generated the internal shell of the granule layer.

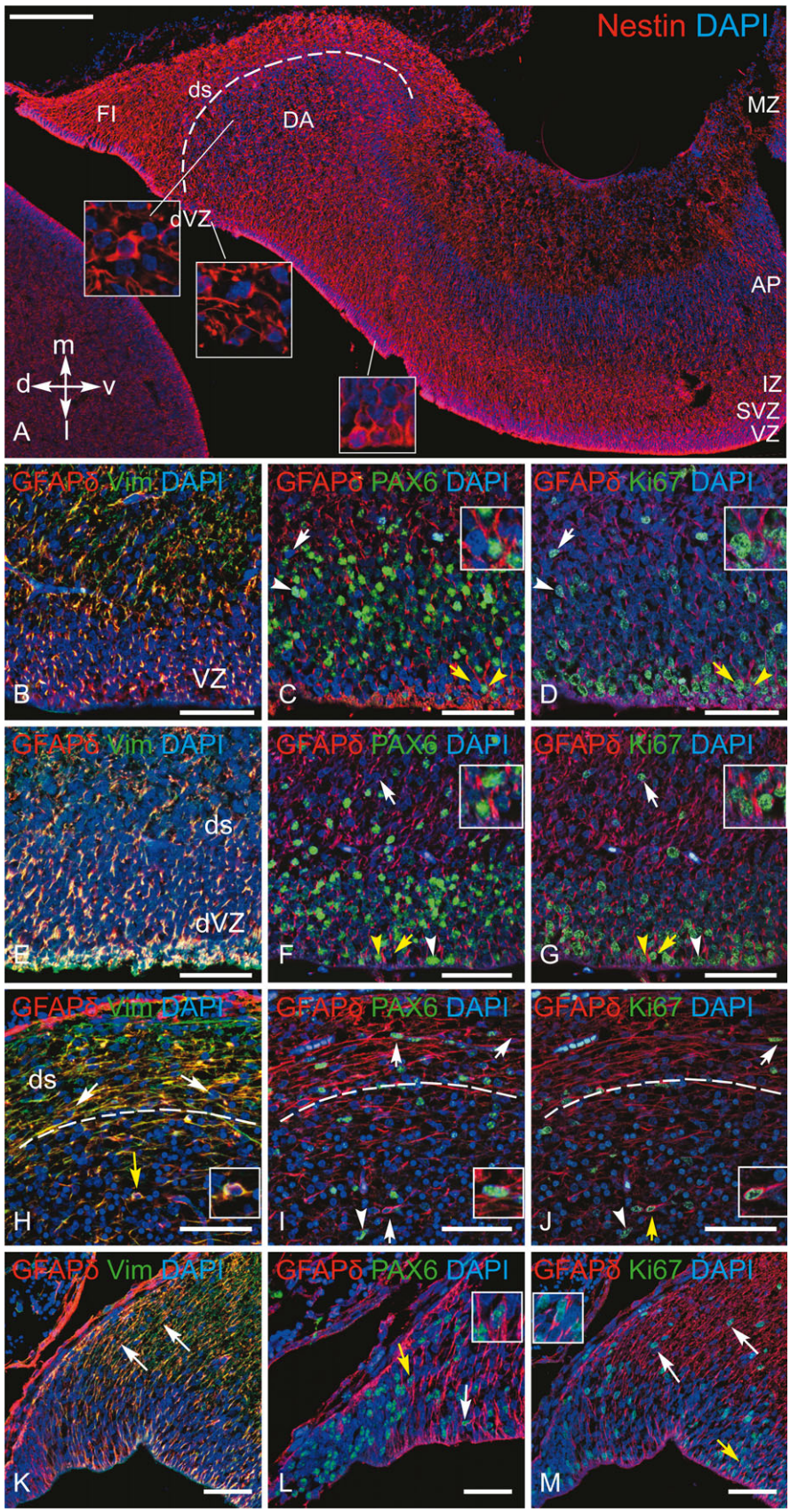


**Figure 1.** Immunolabeling for progenitor cell markers in the hippocampal formation at GW 13. (A): Nestin labeling: insets show the secondary dentate matrix (ds), the dentate anlage (DA), dentate ventricular zone (dVZ) and Ammonic ventricular zone (VZ). In the VZ of Ammon's horn, Nestin$^+$ cells display radial fibers oriented towards the Ammonic plate, typical of apical RGCs. In the dVZ, the cells are less cohesive. In the ds, Nestin$^+$ cells displaying more or less fine processes are present.

### GW 25–30

The pattern of progenitor cell distribution/generation and their neurogenic potential have not been studied beyond GW 20 in Ammon's horn so far. In the dentate area, we have previously reported that, at GW 25, the proliferative activity of PAX6$^+$ progenitor cells is reduced in the hilus and in the secondary dentate matrix, now located at the fimbrio-dentate junction (FDJ) (Cipriani et al. 2017).

At GW 25, we show at present that the VZ of Ammon's horn continues to decrease in thickness. The network of radial glial fibers has begun to degenerate, displaying shorter processes, and star-shaped cells in comparison to previous stages (Fig. 3A,C). Numerous SOX2$^+$ (Supplementary Fig. 3A), Nestin$^+$ (Fig. 3C) and PAX6$^+$ cells (Fig. 3D) were observed in the VZ and SVZ, without detectable colabeling with Ki67 (Fig. 3E). Nestin/GFAPδ colabeling showed the persistence of a few colabeled cells in the VZ and a dense band of tangentially oriented cells and fibers in the SVZ/IZ (Fig. 3C). In parallel, several DCX$^+$ cells were detected above the VZ and in the superficial pyramidal layer (Supplementary Fig. 3B,C), indicating the presence of differentiating neurons within these two compartments.

In the dentate area, Nestin$^+$ cells and fibers were still dense in the SGZ and represented ~50% of the SGZ/hilar population (Fig. 3A). Among numerous SOX2$^+$ (Supplementary Fig. 3D) and PAX6$^+$ cells (~30% of the SGZ/hilar population) (Fig. 3F), a few PAX6$^+$/Ki67$^+$ progenitor cells were detected (~7% of PAX6$^+$ cells) (Fig. 3F). Very few Nestin$^+$ unipolar cells expressed TBR2 (not shown). Among the population of GFAPδ$^+$ cells detected at the FDJ (Fig. 3B, G–J), all of them expressed SOX2 (Fig. 3H), ~70% or 50% expressed PAX6 or Nestin, respectively (Fig. 3I,G), but none of them expressed Ki67 (Fig. 3J). Some PAX6$^+$/Ki67$^+$ progenitor cells were detected in the same area (~2% of PAX6$^+$ cells), (Fig. 3K). Numerous DCX$^+$ cells were located in the hilus and granular layer (Supplementary Fig. 3E,F).

In the fimbria, as in Ammon's horn, PAX6$^+$ glial cells had partially lost their radial organization (Fig. 3L–M). In the upper VZ, GFAPδ$^+$/PAX6$^+$cells sometimes displayed star-shaped morphology or tangential processes oriented toward the internal limb of the DG (Fig. 3L,M). In this last compartment, rare PAX6$^+$/Ki67$^+$ (Fig. 3N) but no GFAPδ$^+$/Ki67$^+$ (Fig. 3M) progenitor cells were detected.

Together these data indicate that neurogenic divisions declined in Ammon's horn between GW 20 and 25, even though DCX$^+$ neurons were detected in the SVZ and the pyramidal layer. In contrast, proliferating progenitor cells remained in the dentate area and fimbria beyond GW 30.

### Perinatal age (GW 38—5 months)

In Ammon's horn, the ependymal layer was labeled for PAX6 (Fig. 4B). GFAP, GFAPδ, and Nestin labeling was detected in some cells of the VZ and SVZ (Fig. 4A,B), and a few double-labeled GFAP$^+$/Nestin$^+$ ependymal cells were observed. The band of GFAP$^+$, Nestin$^+$, and GFAPδ$^+$ cells (Fig. 4A), containing several GFAPδ$^+$/PAX6$^+$ cells and various combinations of GFAP and Nestin labeling persisted in the SVZ (Fig. 4B). A few MCM2$^+$ and Ki67$^+$ cells were present among the SVZ cells (not shown). As observed at the previous stages, proliferative activity was no longer detected using Ki67 in GFAPδ$^+$ (Fig. 4C). However, numerous differentiating neurons, labeled for DCX, were still observed in the SVZ (Fig. 4D) and superficial pyramidal layer (Fig. 4E).

In the dentate gyrus, the subgranular band of Nestin$^+$ RGCs appeared to be reduced in density as compared with previous stages (Fig. 5A, Supplementary Fig. 4B,C), although PAX6 and Nestin were strongly expressed in the SGZ and hilus (Fig. 5C), where they represented more than 30% of the SGZ/hilar cells. Subgranular Nestin$^+$/GFAP$^-$ cells, still displayed unipolar morphology (Supplementary Fig. 4B,C), whereas small cells with short processes were observed in the hilus (Fig. 5D). Numerous star-shaped Nestin$^-$/GFAP$^+$ astrocytes were located in the hilus and SGZ (not shown) as well as a few Nestin$^+$/GFAP$^+$ cells. In contrast, GFAPδ$^+$ cells were almost undetectable (Fig. 5C). Both Nestin$^+$ and PAX6$^+$ cells located near the internal limb of the dentate gyrus partially co-expressed Ki67 (12% and 2%, respectively), (Fig. 5D,E,F). MCM2$^+$/Nestin$^+$ cells were more numerous, some of them located within vessel walls and likely dividing pericytes (not shown). Numerous DCX$^+$ and TUJ1$^+$ neurons represented ~30% of the cells located in the hilus and the GCL (Fig. 5B,G,H, Supplementary Fig. 5).

At the FDJ, ~50% of GFAPδ$^+$ cells co-expressed Nestin and PAX6 (Fig. 4F,H). A few Ki67$^+$ cells were detected, although no colabeling with Nestin was observed (Fig. 4G). Rare DCX$^+$ cells were still detected (Fig. 4I).

In the fimbria, GFAPδ/Nestin (Fig. 4J) and GFAPδ/PAX6 (Fig. 4K) colabeling was reduced in comparison to the mid-gestation stage, as only ~50% of GFAPδ$^+$ cells co-expressed PAX6. In parallel, a few DCX$^+$ cells were still detected (Fig. 4L).

In summary, during the perinatal period, the main proliferative and neurogenic compartment was the dentate gyrus, although the density of Nestin$^+$ RGCs and their proliferative capability were reduced. In parallel, young DCX$^+$ neurons continued to be detected in the Ammonic SVZ and FDJ.

### Childhood 2–10 years

In the Ammonic area, some GFAPδ$^+$/Ki67$^-$ and a few Nestine$^+$/GFAP$^-$ cells were detectable in the SVZ between 2 and 10 years (Fig. 6G). However, DCX$^+$ cells were no longer found in the SVZ or pyramidal layer.

In the dentate gyrus, Nestin labeling was reduced in comparison to the perinatal period, being found in only ~6% of SGZ/hilar cells. Sparse Nestin$^+$ cells with short processes were observed in the molecular layer, SGZ and hilus (Fig. 6A,C). Some of the Nestin$^+$ cells co-expressed Ki67$^+$ (13% of Nestin$^+$ cells at

Dashed line: limit between the DA and ds. (*B*, *E*): Double-labeling for GFAPδ/vimentin. *C*, *D*, *F*, *G*, *I*, *J*: Triple-labeling for PAX6/GFAPδ/Ki67 is split into two figures for each area: GFAPδ/PAX6 colabeling (*C*, *F*, *I*) and GFAPδ/Ki67 colabeling (*D*, *G*, *J*). Arrowheads indicate PAX6$^+$/GFAPδ$^+$/Ki67$^+$ triple-labeled cells and arrows indicate PAX6$^-$/GFAPδ$^+$/Ki67$^+$ double-labeled cells. (*B–D*): In the Ammonic area, GFAPδ$^+$ cells and fibers are present in the VZ, SVZ and IZ. Colabeling for vimentin (*B*), PAX6 (*C*), and Ki67 (*D*; arrowheads) shows that GFAPδ$^+$ cells are proliferating RGCs, located in the VZ, SVZ or IZ. (*E–G*): In the DA, GFAPδ$^+$ cells and fibers are present in the dVZ and the secondary matrix (ds). (*E–G*): Colabeling for vimentin (*E*), PAX6 (*F*) and Ki67 (*G*) (white arrow: PAX6$^-$/Ki67$^+$ cell; white arrowhead: Ki67$^+$/PAX6$^+$ cell, yellow arrow and arrowheads: double-labeled cells shown in the insets). (*H–J*): In the DA, strong GFAPδ/vimentin colabeling is seen in cell bodies and fibers of the ds which tangentially surrounds the DA and coexpress GFAPδ/PAX6 and GFAPδ/Ki67 (white arrows in *H–J*; inset in *I*). The dashed line shows the limit between the DA and the ds. In the core of the DA, basal-like RGCs are less abundant, and colabeled for GFAPδ/vimentin or GFAPδ/Ki67 (arrows: GFAPδ$^+$/Ki67$^+$ cells; arrowheads: PAX6$^+$/Ki67$^+$ cells; yellow arrows: double-labeled cells shown in the insets). (*K–M*). In the fimbria, strong GFAPδ colabeling for vimentin (*K*), PAX6 (*L*) and Ki67 (*M*) is seen (white arrows; yellows arrows: double-labeled cells shown in the insets). Scale bar: A, 200 μm; B–K, 50 μm. d, dorsal; DA, dentate anlage; ds, secondary dentate matrix; dVZ, dentate ventricular zone; FI, fimbria; IZ, intermediate zone; l, lateral; m, medial; MZ, marginal zone; SVZ, subventricular zone; v, ventral, VZ, ventricular zone.

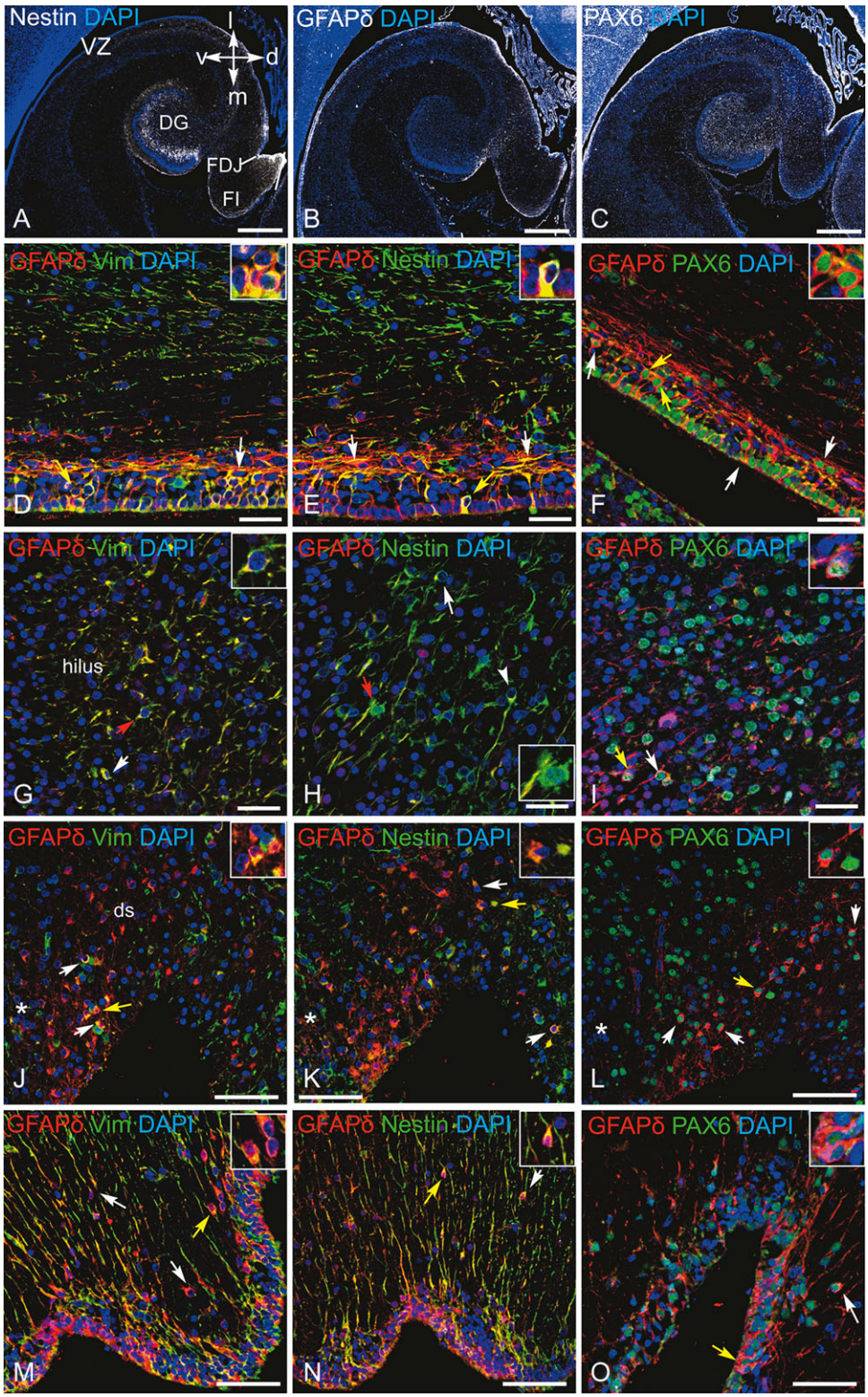


**Figure 2.** Immunolabeling for progenitor cell markers in the hippocampal formation at GW 18. (*A*): Intense Nestin labeling in the molecular layer, the subgranular zone (SGZ) and hilus of the dentate gyrus (DG), the VZ, the fimbrio-dentate junction (FDJ) and the fimbria at low magnification. (*B*): GFAPδ$^+$ cells present along the Ammonic-subicular VZ, in the secondary dentate matrix (ds), the FDJ and the fimbria. They are also present in the DA (see Fig. *G–I* for higher magnification). (*C*): Numerous PAX6$^+$ cells in the Ammonic VZ/SVZ, FDJ, secondary dentate matrix, dentate hilus/SGZ, and fimbria. (*D–F*): In the Ammonic VZ and SVZ, numerous GFAPδ$^+$ RGCs and their fibers are colabeled for vimentin (*D*), Nestin (*E*), and PAX6 (*F*) (arrows; yellow arrows: cells shown in the insets). Note that in the SVZ, RGC fibers are now tangentially oriented toward the pyramidal layer, due to the rotation of the VZ. (*G–I*): Several subtypes of RGCs in the hilus of the dentate gyrus. Unipolar RGCs are radially oriented toward the DG, labeled for vimentin (*G*) and Nestin (*H*) (arrows; red arrows: cells shown in the insets). Many of them are colabeled for GFAPδ$^+$ (arrows in (*G–I*). (*I*): numerous GFAPδ$^+$/PAX6$^+$ cells in the hilus, some of which are shown by arrows. (*J–L*): In the ds and at the FDJ, strongly labeled GFAPδ$^+$ cells are present, some of which are colabeled for vimentin (*J*), Nestin (*K*) and PAX6 (*L*) (arrows; yellow arrows: cells shown in the insets). Asterisk in (*J–L*): internal limb of the granule cell layer. (*M–O*): In the fimbria, GFAPδ strongly labels apical RGCs in the VZ and some RGCs in the upper VZ, partially colabeled for vimentin (*M*), Nestin (*N*) and PAX6 (*O*) (arrows; yellow arrows: cells shown in the insets). Scale bar: *A–C*, 500 μm; *D–N*, 25 μm. d, dorsal; DG, dentate gyrus; ds, secondary dentate matrix; FDJ, fimbrio-dentate junction; l, lateral; m, medial; v, ventral; VZ, ventricular zone.

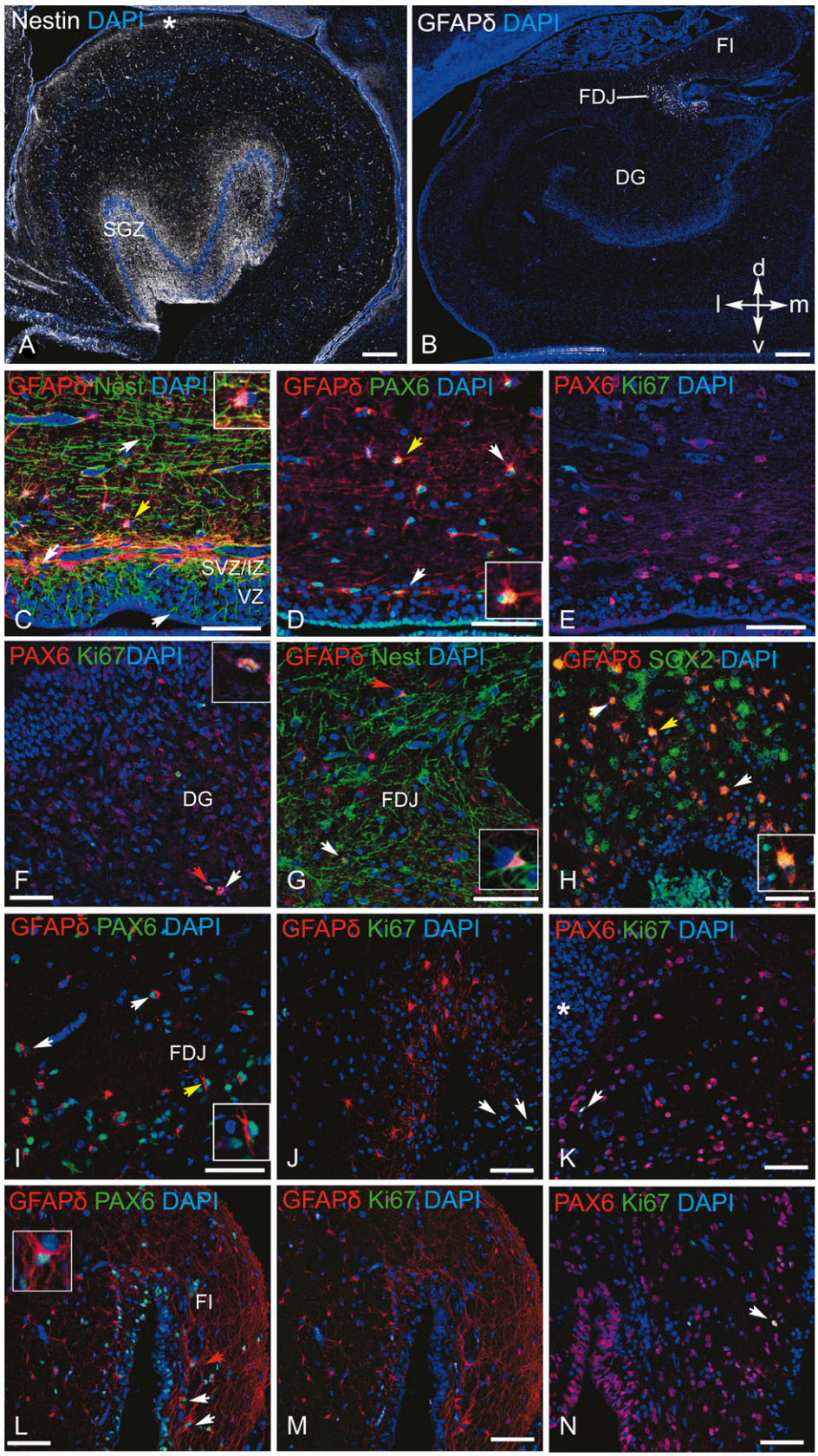


**Figure 3.** Immunolabeling for progenitor cell markers in the hippocampal formation at GW 30. (*A*): Dense Nestin$^+$ cells and fibers in the molecular layer, the subgranular zone (SGZ), the granule cell layer and the hilus. Nestin$^+$ RGCs persist in the Ammonic VZ/SVZ. (*B*): GFAPδ labeling mainly detected at the FDJ (fimbrio-dentate junction). (*C–E*): Labeling in the VZ and SVZ/IZ of the Ammonic plate, (*C*): Nestin/ GFAPδ colabeling showing Nestin$^+$ cells and fibers in the VZ and SVZ/IZ, with some

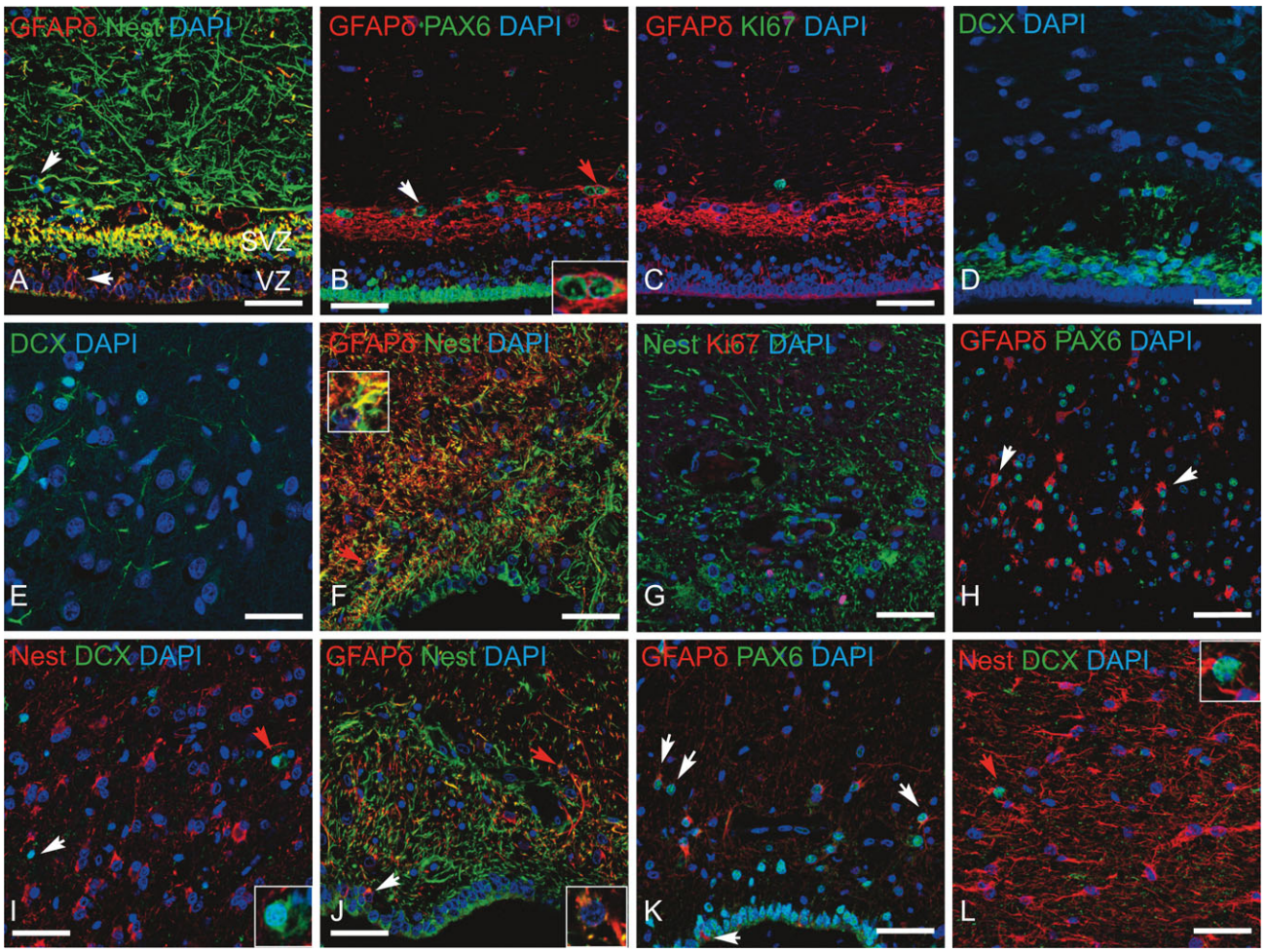


**Figure 4.** Immunolabeling for progenitor cell and neuronal markers in the Ammonic and fimbrial areas during the perinatal period (GW 38—4 months). (*A–D*): In the Ammonic area, Nestin$^+$ cells are present in the VZ and SVZ/IZ (*A*); note the persistence of numerous labeled fibers of GFAPδ$^+$ cells in the VZ and SVZ/IZ. The band of Nestin$^+$/GFAPδ$^+$ labeling also persists. Some GFAPδ$^+$ cells colabeled for Nestin (*A*; arrow) or PAX6 (*B*; arrows; red arrow: cells shown in the inset) but not with Ki67 (*C*). (*D*, *E*): Doublecortin$^+$ (DCX$^+$) cells in the SVZ (*D*) and in the superficial pyramidal layer (*E*). (*F–I*): In the fimbrio-dentate junction, numerous Nestin/GFAPδ colabeled cells and fibers (*F* and insert). (*G*): Numerous Nestin$^+$ cells, a few of which are double-labeled for Ki67$^+$. (*H*): Some GFAPδ$^+$ cells colabeled for PAX6. (*I*): Some DCX$^+$ cells. (*J–L*): In the fimbria, dense Nestin$^+$ cells, some of them colabeled for GFAPδ (*J*; arrow) intermingled with DCX$^+$ cells (*L*). (*K*): PAX6/GFAPδ colabeling in the VZ and upper VZ (arrows). Scale bar: 50 μm.

2 years) (Fig. 6*A*,*C*), and detected in the SGZ until 10 years of age (Fig. 6*I*). MCM2 expression was detected in more cells than Ki67 (not shown). GFAP$^+$ astrocytes were present, but GFAPδ$^+$ cells were rare and displayed an astrocyte-like morphology without detectable Ki67 expression (Fig. 6*D*). In parallel, DCX$^+$/TUJ1$^+$ cells were still present in the GCL at 2 years (~5% of the cells) (Fig. 6*B*,*E*), although their density appeared to decrease at 5 years and they were not detectable at 7 and 10 years (Fig. 6*J*).

At the FDJ and fimbria, star-shaped Nestin$^+$ and/or GFAPδ$^+$ cells with no detectable Ki67-labeling appeared (Fig. 6*F*,*H*,*K*).

Together these data show a decline in progenitor cell density while young neurons are still generated in the dentate gyrus during childhood.

## Markers of progenitor cells and young neurons in subjects without neurological disorders (23–65 years)

The distribution and semi-quantitative evaluation of Nestin$^+$ and GFAPδ$^+$ cells are summarized in Table 5. Nestin labeling intensity and cell density were highly variable both in the SVZ and the dentate gyrus. GFAP$^+$ astrocytes were abundantly present.

In the Ammonic area of controls, star-shaped Nestin$^+$ cells resembling astrocytes were detected in the SVZ of nine individuals and appeared numerous in five cases older than 45 years (Fig. 7*A*,*B*, Supplementary Fig. 5A). GFAPδ$^+$ cells (8/11 cases) displaying a similar morphology were more abundant in seven

colabeled cells (arrows: yellow arrows: cells shown in the insets). (*D*): Numerous PAX6$^+$ cells in the VZ and some in the SVZ, sometimes colabeled for GFAPδ (arrows; yellow arrows: cells shown in the insets). (*E*): A Ki67$^+$/PAX6$^-$ cell in the SVZ/IZ. (*F*): Rare PAX6$^+$/Ki67$^+$ cells in the dentate hilus (red arrow: double-labeled cell shown in the inset). (*G–K*): In the FDJ, GFAPδ/Nestin double-labeling shows numerous Nestin$^+$ cells and some colabeled cells (*G*) (arrows; red arrow: cell shown in the inset). Numerous GFAPδ$^+$ cells colabeled for SOX2 (*H*) and PAX6 (*I*) (arrows; yellow arrow: cell shown in the inset), but not for Ki67 (*J*; arrow). (*K*): Rare PAX6$^+$/Ki67$^+$ cells (arrow) near the internal limb of the granule cell layer (asterisk). (*L–N*): In the fimbria (FI), GFAPδ$^+$ cells and fibers in the upper VZ, some of which are colabeled for PAX6 (*L*; arrows; red arrow: cell shown in the inset) but not for Ki67 (*M*). (*N*): Numerous PAX6$^+$ cells in the VZ and upper VZ, with rare PAX/Ki67 colabeling (arrow). Scale bar: *A*, *B*, 500 μm *C–L*, 50 μm. d, dorsal; DG, dentate gyrus; FI, fimbria; FDJ fimbrio-dentate junction; l, lateral; m, medial; SGZ, subgranular zone; v, ventral.

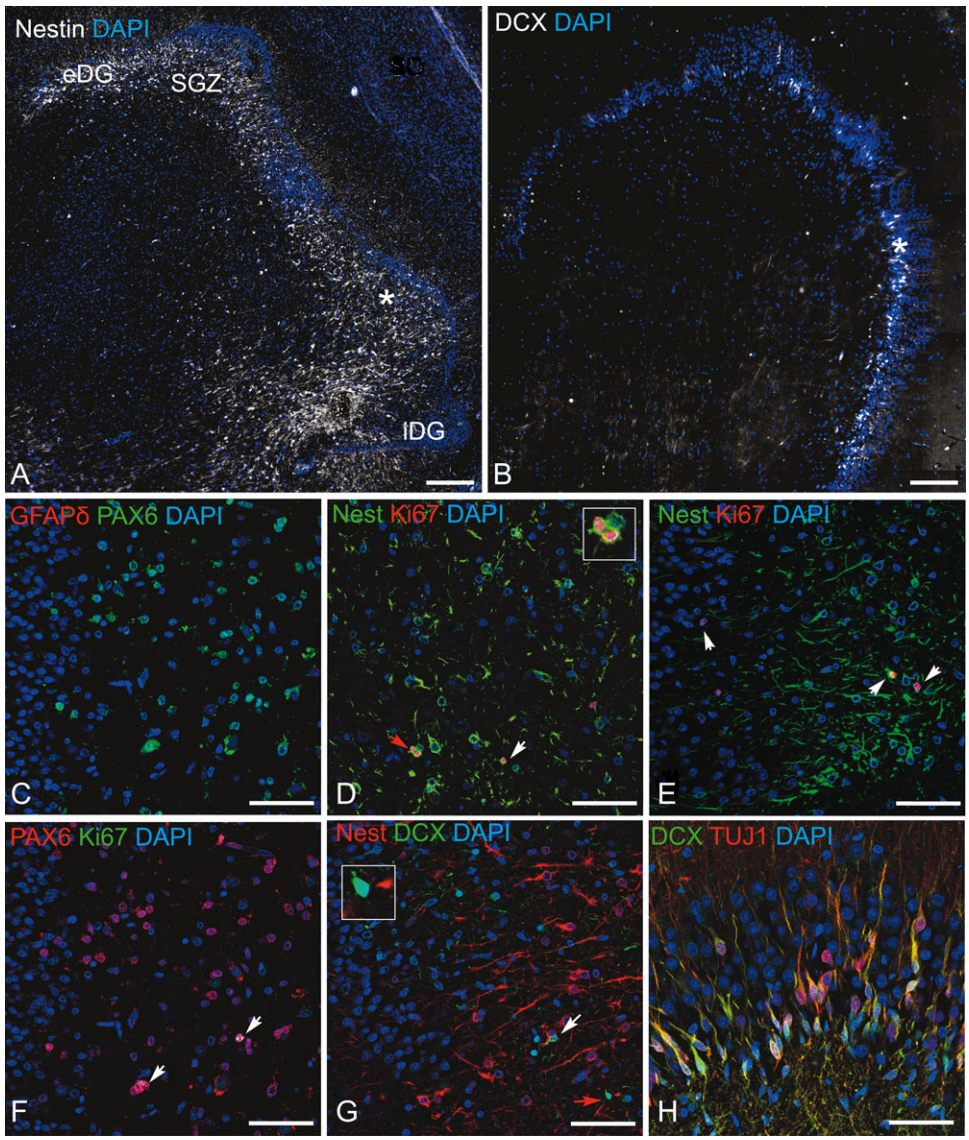


**Figure 5.** Immunolabeling for progenitor cell and neuronal markers in the dentate gyrus during the perinatal period (GW 38—4 months). (*A*,*B*): Persistence of Nestin$^+$ RGCs (*A*) and DCX$^+$ neurons (*B*) in the subgranular zone (SGZ). Both cell types are denser in the internal limb (iDG) of the granule cell layer than in the external limb (eDG). (*C*): Numerous PAX6$^+$ cells in the hilus but with no GFAPδ labeling. *D*, *E* (*E*: higher magnification of the region indicated by the white asterisk in *A*): Nestin$^+$/Ki67$^+$ cells in the granule cell layer, SGZ and the hilus of the dentate gyrus, mainly located near the iDG. Numerous Nestin$^+$ cells still display unipolar radial process. (*F*): numerous PAX6$^+$ cells and rare PAX6$^+$/Ki67$^+$ cells near the iDG (arrows). (*G*): Several DCX$^+$ cells close to the iDG (arrows; red arrow: cells shown in the inset). (*H*): numerous DCX$^+$/TUJ1$^+$ double-labeled cells mainly located in the SGZ and deep granular layer at 4 months. eDG, external limb of the dentate gyrus; iDG, internal limb of the dentate gyrus; SGZ, subgranular zone; Scale bars: *A*, *B*, 500 μm; *C*–*H*, 25 μm.

controls (Fig. 7*B*,*C*). GFAP/Nestin and GFAPδ/Nestin co-expression was infrequently seen (Fig. 7*B*). Although rare Ki67$^+$ cells and some MCM2$^+$ cells were detected, no Ki67/Nestin, Ki67/GFAPδ, or MCM2$^+$/Nestin colabeling was observed (Fig. 7*A*,*C*). Nestin$^+$ and GFAPδ$^+$ cells were detected in ependymal granulations of seven and nine control cases, respectively.

In the dentate gyrus, very few Ki67$^+$ cells were detected (between 0 and 2 in the total area of the GCL/SGZ, although a 23 years-old drug addict control who died from a spetic shock had 1.1 Ki67$^+$ cells/mm of SGZ length, near to the values observed during the perinatal period). MCM2$^+$ cells were more numerous although their density varied highly between cases. Nestin$^+$ cells were observed in nine controls, predominantly in the SGZ and hilus compared with the GCL. They displayed a star-shaped morphology or a few long processes extending through the granular layer or the hilus (Fig. 7*D*,*F*, Supplementary Figs 4*D*, *E* and 6*B*–*D*). Their cell bodies or processes were more or less in contact with vessels (Fig. 7*D*,*E*). In the same areas, rare Nestin$^+$ cells displaying bipolar/unipolar or short processes were detected. Among them, in one case, a Nestin$^+$ cell co-expressing Ki67 was observed (Fig. 7*F*), and a few MCM2$^+$/Nestin$^+$ cells were observed in the vascular wall (not shown). Nestin$^+$ cells inconsistently co-expressed GFAP. GFAPδ$^+$ cells were not observed in the dentate gyrus of young adult cases (23–41 years). In older cases (45–65-year-old), GFAPδ$^+$ cells displayed astrocyte-like morphologies, and were sometimes opposed to vessel walls (Fig. 7*H*). Less than 30% of GFAPδ$^+$ cells were colabeled for Nestin (Fig. 7*G*,*H*), and none for Ki67 (Fig. 7*I*). SOX2, PAX6, and TBR2

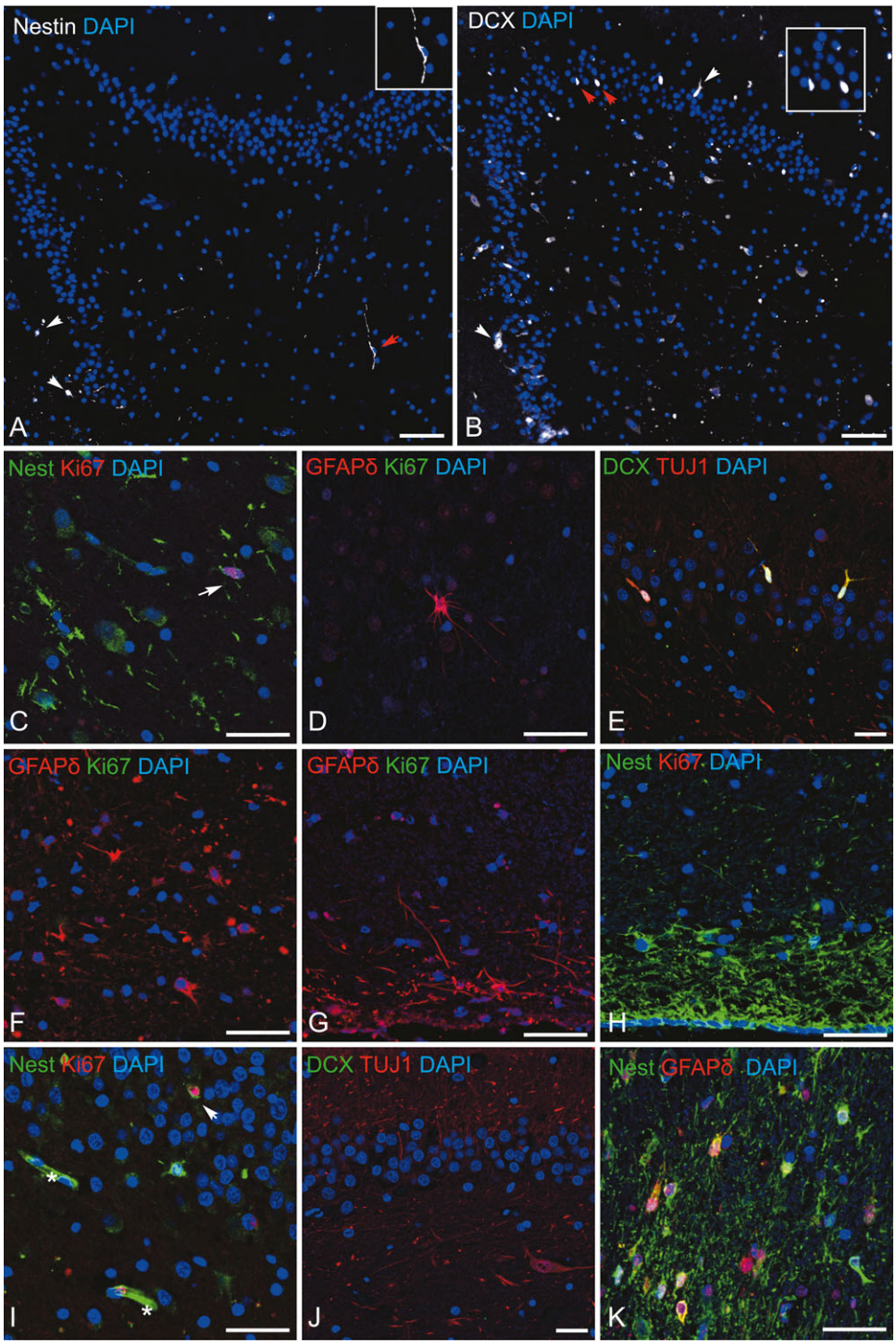


**Figure 6.** Immunolabeling for progenitor and neuronal cell markers in the hippocampal formation during childhood (2–10 years). (*A–H*): 2-year-old and (*I–K*): 10-year-old hippocampi. *A*, *B*: Sparse Nestin$^+$ (*A*) and numerous DCX$^+$ cells (*B*; arrows; red arrow: cells shown in the inset) are still present, and are denser close to the internal limb of the dentate gyrus, on the left. (*C*, *D*): Nestin$^+$/Ki67$^+$ cells (*C*; arrow) and GFAPδ$^+$/Ki67$^-$ cells (*D*) in the hilus of the dentate gyrus. (*E*) Ramified DCX$^+$/TUJ1$^+$cells in the dentate granular layer. (*F*): Numerous GFAPδ$^+$/Ki67$^-$ cells are still detected at the fimbrio-dentate junction. (*G*): GFAPδ$^+$/Ki67$^-$ cells in the Ammonic SVZ. (*H*): Nestin$^+$/Ki67$^-$ cells in the fimbria. (*I*): A few Nestin$^+$ and Nestin$^+$/Ki67$^+$ cells in the dentate gyrus (arrow; asterisks: two Nestin$^+$ vessels, note the presence of one Nestin$^+$/Ki67$^+$ cell). (*J*): No DCX/TUJ1 labeling in the granule cell layer. (*K*): Nestin$^+$ and/or GFAPδ$^+$ cells at the fimbrio-dentate junction. Scale bar: *A*, *B*, 100 μm; *C*, *D*, *F–I* and *K*, 20 μm; *E* and *J*, 10 μm.

**Table 5.** Distribution of GFAPδ and Nestin immunoreactive cells in adult hippocampi in subjects with and without Alzheimer's disease

| Cases | Age | Gender | SVZ | | GCL | | SGZ/Hilus | | Fimbria | | FDJ | | Subpial layer | | | EG | |
|---|---|---|---|---|---|---|---|---|---|---|---|---|---|---|---|---|---|
| | | | Nestin | GFAPδ | Nestin | GFAPδ | Nestin | GFAPδ | Nestin | GFAPδ | Nestin | GFAPδ | | Nestin | GFAPδ | Nestin | GFAPδ |
| Controls | | | | | | | | | | | | | | | | | |
| A112-06–28 | 23 | M | + | – | + | – | + | – | +++ | – | + | NA | – | | ++ | +++ | NA |
| A46-12-5 | 29 | M | – | – | + | – | + | +++ | – | + | ++ | – | | ++ | + | +++ | |
| A12-021 | 41 | M | + | ++ | – | – | – | + | – | NA | NA | – | | – | + | + | |
| A1178 | 45 | M | ++ | +++ | ++ | – | ++ | +++ | +++ | ++ | ++ | +++ | ++ | | ++ | +++ | – |
| A13-56 | 47 | M | + | ++ | – | – | +++ | +++ | +++ | ++ | | NA | +++ | | ++ | NA | +++ |
| A14-3 | 51 | F | ++ | +++ | +++ | – | +++ | +++ | +++ | +++ | +++ | ++++ | +++ | | +++ | +++ | + |
| A11-046 | 52 | F | +++ | ++++ | + | – | ++ | ++ | +++ | NA | | +++ | +++ | | ++ | NA | ++++ |
| A1430 | 54 | M | + | ++ | – | + | ++ | + | ++ | + | + | – | | ++ | + | +++ | |
| A14-23 | 54 | F | ++ | +++ | + | – | + | ++ | ++ | ++ | +++ | +++ | ++ | | ++ | ++ | ++ |
| A11-073 | 61 | F | – | – | – | – | + | – | ++ | +++ | | ++ | – | | – | NA | |
| A11-066 | 65 | M | ++ | + | – | – | – | ++ | ++ | +++ | | NA | – | | ++ | NA | +++ |
| AD | | | | | | | | | | | | | | | | | |
| A1297 | 74 | F | +++ | ++ | + | – | ++ | + | NA | NA | ++ | + | – | | – | – | + |
| A1264 | 78 | M | + | ++ | + | – | + | ++ | + | ++ | ++ | ++ | – | | – | + | ++ |
| A1238 | 79 | M | + | ++ | – | – | – | ++ | NA | NA | + | +++ | – | | – | + | + |
| A1274 | 86 | M | + | +++ | – | – | + | ++ | ++ | NA | + | NA | – | | + | + | ++ |
| A1254 | 89 | M | + | +++ | ++ | – | ++ | ++ | – | + | + | ++ | + | | + | NA | ++ |

EG, ependymal granulations; FDJ, fimbrio-dentate-junction; GCL, granular cell layer, SGZ, subgranular zone; SVZ, subventricular zone.

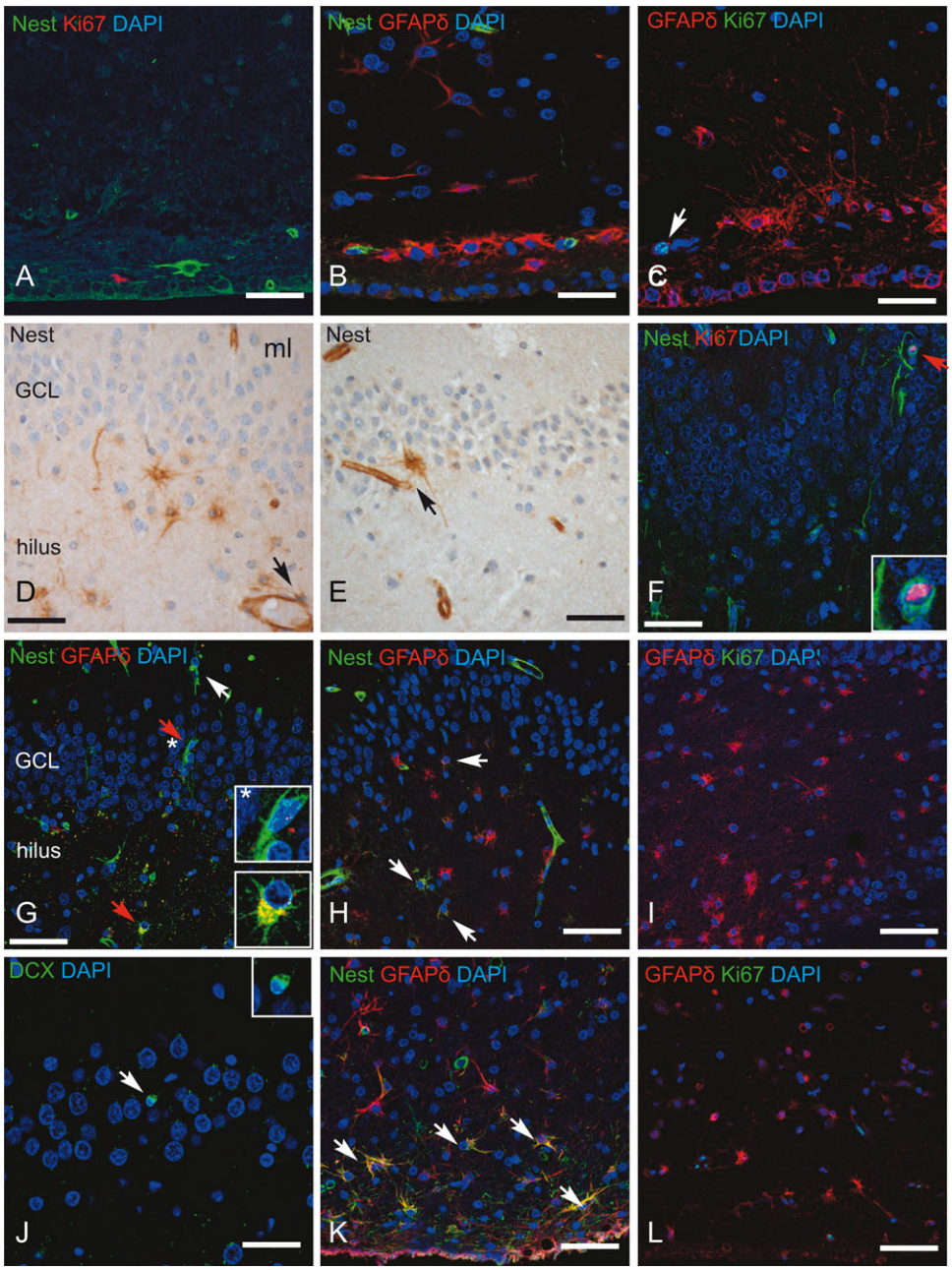


**Figure 7.** Immunolabeling for progenitor and neuronal cell markers in the adult hippocampal formation of control donors. (*A–C*): Ammonic area. (*A*): A few Nestin$^+$/Ki67$^-$ cells in the SVZ of a 41-year-old donor; note that some ependymal cells are weakly labeled. (*B*): Numerous GFAPδ$^+$ cells associated with a few Nestin$^+$ cells in the SVZ of a 51-year-old donor. (*C*): GFAPδ $^+$/Ki67$^-$ cells in the SVZ of a 54-year-old donor; the arrow shows a GFAPδ$^-$/Ki67$^+$ cell. (*D–J*): dentate gyrus. (*D*, *E*): Nestin$^+$ cells in the subgranular zone (SGZ) of a 54-year-old and a 51-year-old donor, respectively. Note the presence of Nestin$^+$ cells in contact with the vessel wall through their endfeet (arrows in *D* and *E*). (*F*): A Nestin$^+$ cell with a long fine process running into the granule cell layer and a Nestin$^+$/Ki67$^+$ cell surrounded by Nestin$^+$ fibers in the granule cell layer (red arrow and inset). (*G*): A 45-year-old donor. Nestin$^+$/GFAPδ$^-$ cells displaying unipolar or bipolar processes in the molecular layer (white arrow) and granule cell layer (GCL; red arrow and upper inset). Star-shaped Nestin$^+$/GFAPδ$^-$ and Nestin$^+$/GFAPδ$^+$ cells in the hilus (red arrow and lower inset). (*H*): In a 51-year-old donor, star-shaped Nestin$^-$/ GFAPδ$^+$ and Nestin$^+$/GFAPδ$^+$ cells in the SGZ and hilus (arrows), note the presence of Nestin$^-$/ GFAPδ$^+$ cells apposed to vessels. (*I*): Numerous GFAPδ$^+$/Ki67$^-$ cells in the hilus and SGZ of a 79-year-old control. (*J*): One DCX$^+$ cell in a 61-year-old donor. (*K*, *L*): the fimbria of a 54-year-old donor. (*K*): Numerous star-shaped GFAPδ$^+$/Nestin$^+$ (arrows) and GFAPδ$^+$/Nestin$^-$ cells. (*L*): GFAPδ/Ki67 colabeling was not detected. GCL, granule cell layer. Scale bar: *A–C* and *J*, 12 μm; *D–I*, and *K*, *L*, 25 μm.

immunoreactivity was not detected (not shown). At all ages, we observed DCX$^+$ cells (> 1% of GCL cells) displaying scanty cytoplasm, both in the hilus and the SGZ (Fig. 7*J*).

The FDJ/fimbria showed variable numbers of Nestin$^+$ cells with long or short processes (Fig. 7*K*, Supplementary Fig. 6*E*,*F*, Table 5). Numerous GFAPδ$^+$ (Fig. 7*K*,*L*) cells were also observed (Table 5). Some GFAPδ$^+$ cells in the upper VZ were colabeled for Nestin (Fig. 7*K*) but not for Ki67 (Fig. 7*L*).

Together these data indicate that different morphologies of Nestin$^-$ and/or GFAPδ-expressing cells lacking significant proliferative activity were observed in the SVZ, dentate gyrus, and FDJ/fimbria of the adult hippocampus.

### Markers of progenitor cells and young neurons during pathological aging

In the SVZ of patients with AD, a few Nestin$^+$ cells were detected, with only one case displaying dense Nestin labeling (Fig. 8*A–C*, Table 5). GFAPδ$^+$ cells were more numerous than Nestin$^+$ cells in all the cases (Fig. 8*B–D*, Table 5), and sometimes overlaid the Nestin labeling (Fig. 8C). In one case, a proliferating GFAPδ$^+$/Ki67$^+$ cell was detected (Fig. 8D).

In the dentate gyrus, the density of Nestin-labeled cells varied among cases. In four cases, round cells with few processes or star-shaped Nestin$^+$ cells were detected in the granular layer, SGZ (Fig. 8*E*,*F*,*G*,*H* and Supplementary Fig. 4*F*) and molecular layer (Fig. 8*I*). Cells with long radial processes were also seen (Fig. 8*E*,*J*). Both cell types sometimes co-expressed GFAPδ (Fig. 8*H–J*). GFAPδ$^+$ cells were observed in the hilus of all the cases and were more abundant than Nestin$^+$ cells (Fig. 8*H*,*K* and Table 5). Both Nestin$^+$ and GFAPδ$^+$ cells lacked proliferative activity as detected using Ki67 labeling (Fig. 8*G*,*K*). In the few AD cases, in contrast to control cases, we did not detect any obvious close contacts between Nestin$^+$ and/or GFAPδ$^+$ cells and vessels (Fig. 8*E–K*). SOX2 immunoreactivity was not detected (not shown).

In the FDJ/fimbria, star-shaped Nestin$^+$ (Fig. 8*L*,*M*) and GFAPδ$^+$ cells (Fig. 8*N*,*O*) were detected, but no GFAPδ/Nestin (Fig. 8*N*) or GFAPδ/Ki67 (Fig. 8*O*) colabeling was observed.

Taken together, these observations indicate the persistence of Nestin$^+$ and/or GFAPδ$^+$ cells in the hippocampal SVZ, dentate gyrus and FDJ/fimbria of patients with AD. Moreover, in the granular layer and SGZ, Nestin$^+$ cells with long radial processes resembling developmental RGCs were still observed. Close contacts between Nestin$^+$ and/or GFAPδ$^+$ cells and vessels were less obvious compared with control cases.

## Discussion

This is the first study to investigate progenitor cell subtypes and their neurogenic potential in the human hippocampus from fetal development to adulthood, in subjects without neurological disorders and AD patients. Our results indicate that:

- In the dentate anlage, between GW 13 and 16, the secondary matrix gives rise to a third proliferative matrix within the hilus and the SGZ, whose proliferation and neurogenic potential decrease from GW 25 onward; however, proliferating progenitor cells with neurogenic potential persist in the dentate gyrus until childhood and DCX$^+$ cells are detected until 5 years. A few DCX$^+$ cells are present in adults. In the pyramidal layer and SVZ, DCX expression persists only until the early perinatal period indicating that the cell proliferation potential in the dentate gyrus lasts longer than in the Ammonic-subicular regions (Cipriani et al. 2016).
- The outer shell of the GCL is mainly formed by the secondary dentate matrix, whereas the inner shell is formed at later stages by the tertiary matrix, as suggested by animal studies (Altman and Bayer 1990a,1990b).
- Putative resting stem cells were observed in the SVZ, dentate gyrus and FDJ/fimbria of the adult human hippocampus from controls and patients with AD, but they lacked significant proliferative activity.
- Hippocampal RGCs at these different stages are morphologically, topographically, and antigenically heterogeneous. The putative NPC marker GFAPδ is expressed in RGCs of the human hippocampal formation during development.

### RGC subtypes and their neurogenic potential in the ammonic fields during development and aging

During development, progenitor cell markers (Nestin, vimentin, PAX6, and GFAPδ) reveal two subtypes of RGCs in the ammonic matrices: apical RGCs in the VZ and basal-like RGCs in the SVZ/IZ. We observed colabeling with variable levels of these markers across the lifespan. In particular, RGCs were highly colabeled for Nestin and GFAPδ at early stages of development, whereas around mid-gestation, various patterns of single- or double-labeling appeared. Despite the morphological resemblance of hippocampal RGCs to neocortical RGC described in humans (Hansen et al. 2010) and non-human primates (Betizeau et al. 2013), we have previously reported differences in the pattern of pyramidal neuron lamination in various hippocampal regions (i.e. Ammon's horn, the subicular complex, and the entorhinal cortex) (Cipriani et al. 2016), indicating the molecular heterogeneity of RGCs. The characterization of RGCs in these areas could provide crucial information about the mechanisms involved in neuronal subtype specification, lamination, and areal specification in the hippocampus as compared with the neocortex.

The neurogenic potential of RGCs has been shown to decrease from GW 20 (Cipriani et al. 2016) in the Ammonic VZ. However, PAX6$^+$ cells remain abundant in the VZ/ependymal layer and SVZ until the perinatal period. Despite the low proliferation detected using Ki67 and MCM2 beyond GW 25, DCX$^+$ cells are detectable until the early perinatal period in the SVZ and the pyramidal layer. One cannot exclude the possibility that immature neurons remain for a longer period of time in the SVZ/IZ and deep pyramidal layer before differentiating into mature neurons (Altman and Bayer 1990c), or in another scenario, that cell cycling does occur and some late-generated neurons are destined to migrate out of the hippocampus. Sanai et al. (2011) have reported the presence of migrating immature neurons in the SVZ of the lateral ventricles and the rostral migratory stream in infants before 18 months of age, a phenomenon that subsides in older children. In addition, a major migratory pathway in these infants targets the prefrontal cortex (Sanai et al. 2011). In contrast, the fate of hippocampal SVZ neurons remains to be established.

In adults, a ribbon of GFAP$^+$, GFAPδ$^+$, and Nestin$^+$ cells displaying astrocyte-like morphology persists in the SVZ. One GFAPδ$^+$/Ki67δ$^+$ cell was observed, in the SVZ of a patient with AD. The distribution and the morphology of GFAPδ$^+$ and Nestin$^+$ cells in hippocampal SVZ of AD patients is overall similar to that of controls, confirming previous studies on GFAPδ (Roelofs et al. 2005; Kamphuis et al. 2014). Moreover, the number of GFAPδ$^+$ cells in the SVZ of the lateral ventricle does not appear to be affected in other neurodegenerative diseases (van den Berge et al. 2011). We observed variable GFAP/Nestin and GFAPδ/Nestin colabeling, in agreement with previous observations in the lateral ventricles (van den Berge et al. 2010) and temporal lobe (Liu et al. 2018). GFAP$^+$ and/or Nestin$^+$ labeled cells are observed in ependymal granulations in our adult subjects and may represent regenerative "reactive astrocytes". However, the properties of these GFAP$^+$ and/or Nestin$^+$ and GFAPδ and/or Nestin$^+$ cells are not clear, as few reports are available. Nestin-expressing cells increase in density in the temporal lobe during epilepsy (Liu et al. 2018). Weak Nestin expression is observed in occasional astrocytes in the normal white matter, and increases in "reactive astrocytes" in acute and chronic plaques in multiple sclerosis (Holley et al. 2003). Roelofs et al. have reported that GFAPδ expression is not associated with gliosis in patients with multiple sclerosis. GFAPδ

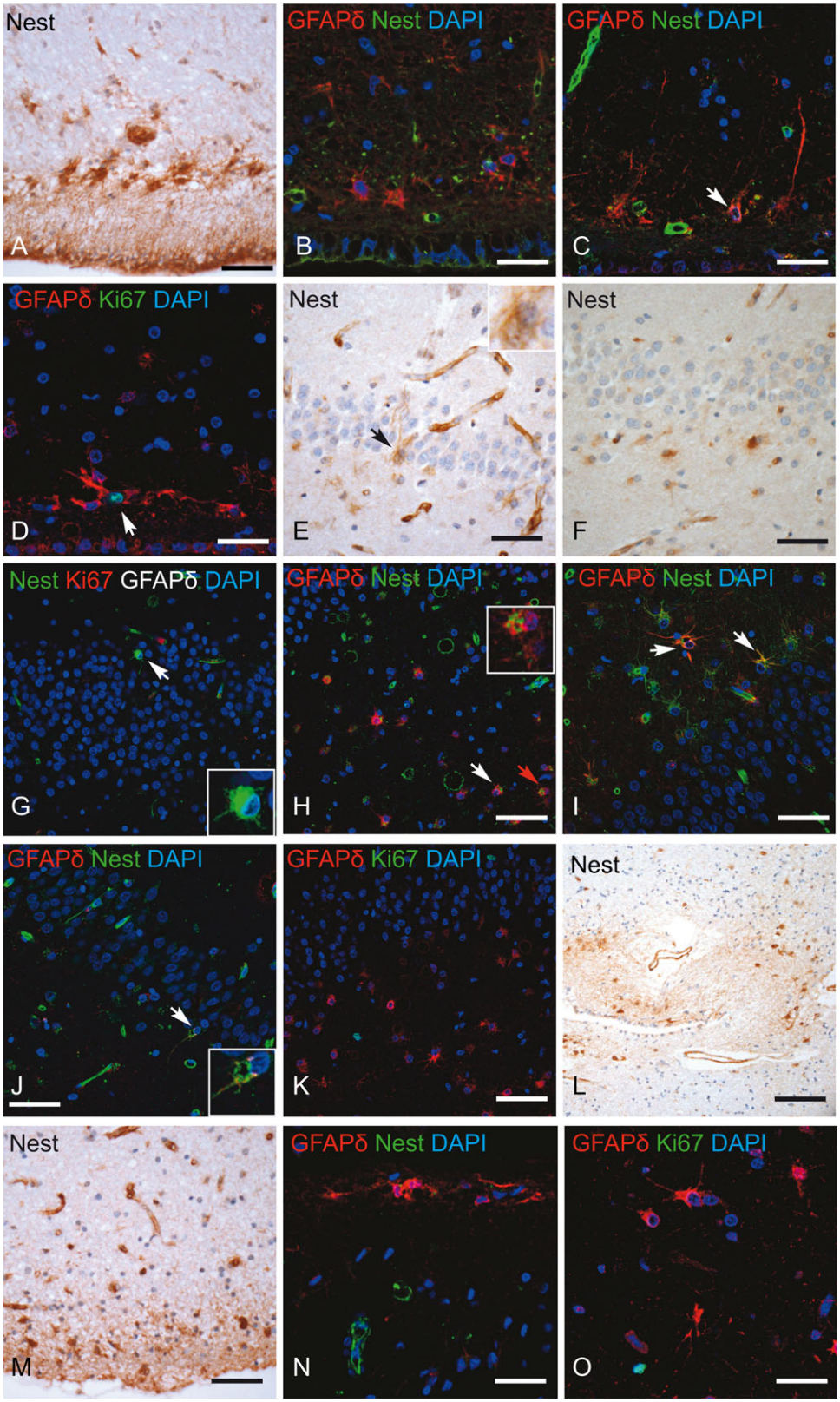


**Figure 8.** Immunolabeling for progenitor and neuronal cell markers in the adult hippocampal formation of patients of different ages with Alzheimer's disease: 74 years (*A*, *E*), 78 years (*F*, *G*, *J*, *N*), 79 years (*B*, *C*, *H*, *K*, *O*), 86 years (*I*, *L*, *M*) and 89 years (*D*). (*A*–*D*): Ammonic compartment. a: Nestin labels ependymal cells and numerous cells in the SVZ in one case. (*B*): GFAPδ$^+$ cells are more abundant than Nestin$^+$ cells, but there is no colabeling. (*C*): One GFAPδ/Nestin colabeled cell (arrow). (*D*): A GFAPδ$^+$/Ki67$^+$ cell in the SVZ (arrow). (*E*–*K*): dentate gyrus. (*E*, *F*): star-shaped Nestin$^+$ cells in the granule cell layer (GCL), subgranular zone (SGZ) and the hilus. Note the presence of 2 cells in the GCL bearing long processes in *E* (arrow). (*G*): Nestin/Ki67/GFAPδ triple-labeling showing a round Nestin$^+$ cell with a few short processes (arrow and inset). No colabeling is seen. (*H*, *I*): GFAPδ/Nestin colabeling showing Nestin$^+$ cells and double-labeled cells in the hilus and SGZ (red arrow and inset in *H*), and in the GCL and molecular layer (arrows in *I*). (*J*): a GFAPδ$^+$/Nestin$^+$ cell with long fine radial processes in the GCL (arrow and inset). A GFAPδ$^-$/Nestin$^+$ cell with a long fine process is seen at the top of the panel. (*K*): GFAPδ$^+$/Ki67$^-$ cells located in the SGZ and the hilus. (*L*, *N*, *O*): In the fimbria, numerous Nestin$^+$ and GFAPδ$^+$ cells are present (*L*), but without colabeling (*N*), and GFAPδ$^+$ cells do not show detectable proliferative activity (*O*). (*M*): Nestin labeling showing numerous cells at the fimbrio-dentate junction. Scale bar: *A*–*F* and *L*–*M*, 12 μm; *J*, *K*, 25 μm.

might play a role in modulating intermediate filament cytoskeletal properties, possibly facilitating astrocyte motility (Roelofs et al. 2005). Alternatively, several studies suggest that human SVZ astrocytes lining the lateral ventricles are quiescent neural stem cells (Sanai et al. 2004; Leonard et al. 2009; van den Berge et al. 2010) that express vimentin, GFAP and GFAPδ (Sanai et al. 2004; Roelofs et al. 2005; Leonard et al. 2009; van den Berge et al. 2010) and behave as multipotent progenitor cells *in vitro* (Sanai et al. 2004; Leonard et al. 2009; van den Berge et al. 2010). Interestingly, GFAPδ/Nestin colabeling is observed in neurospheres prepared from the adult human SVZ (van den Berge et al. 2010).

We did not detect DCX$^+$ neurons in the adult ammonic area, in agreement with previous observations in lateral ventricles (Sanai et al. 2011). Therefore, further studies will be required to elucidate whether the hippocampal SVZ can be considered as a neurogenic niche in adult humans.

## RGC subtypes and their neurogenic potential in the dentate anlage during development and up to the perinatal period

The mechanisms of the formation of the dentate matrices are not well understood. We have previously shown the sequential formation of dentate matrices from GW 10 to 25 (Cipriani et al. 2017).

Here we show that at GW 13, the secondary dentate matrix is formed by PAX6$^+$/Nestin$^+$/GFAPδ$^+$ unipolar and multipolar tangentially oriented RGCs, extending from the IZ to the subpial region and surrounding the cluster of nascent post-mitotic granule neurons in the dentate anlage (Cipriani et al. 2017). Our data strongly support previous experimental studies suggesting that this secondary dentate matrix is the source of the outer shell of the dentate gyrus (Altman and Bayer 1990b). Around GW 16, the hilar matrix and the SGZ become identifiable, containing highly proliferative and unipolar PAX6$^+$/Nestin$^+$/GFAPδ$^+$ RGCs bearing radially oriented processes that extend through the granule cell and molecular layers. We have previously shown that granule neurons migrate in an outside-in pattern (Cipriani et al. 2017). Overall, our results are in line with the radial unit hypothesis proposed in primates (Eckenhoff and Rakic 1984), and experimental data suggesting that the inner shell of the dentate gyrus is derived from the SGZ and hilar matrix (Altman and Bayer 1990b). From mid-gestation, the expression pattern of neural stem/progenitor cell markers changes. Progenitor cells remain strongly immunoreactive for Nestin while GFAPδ labeling predominates in the secondary dentate matrix and FDJ/fimbria. Our data show that Ki67$^+$ and MCM2$^+$ proliferating dentate progenitor cells and neurogenesis decline in the human dentate gyrus from 25 GW. Around the perinatal period, the dense network of RGCs in the SGZ starts to decrease in density, but neurogenesis persists during childhood until 5 years.

## Neurogenic potential in the dentate gyrus during normal adulthood

The study by Eriksson et al. (1998) has raised a great amount of interest in the potential mechanisms involved in adult human dentate neurogenesis. Here, we demonstrate the expression of Nestin and/or GFAPδ in the dentate gyrus of most adults, confirming previous studies (Roelofs et al. 2005), Some of the Nestin$^+$ and/or GFAPδ$^+$ cells in our study contacted vessel walls through their somata or cell processes, resembling astrocytic endfeet. These may represent a vascular niche of stem cells, as reported in the adult rodent dentate gyrus (Palmer et al. 2000; Shen 2004; Tavazoie et al. 2008).

The variable degree of expression and colabeling of GFAP/Nestin and Nestin/GFAPδ, as shown in the present and in a previous paper (Liu et al. 2018), suggests the presence of antigenically heterogeneous cells with putative stem cell properties (Decarolis et al. 2013). Moreover, in addition to cells with an astrocytic morphology, we observed a few bipolar/unipolar Nestin$^+$ cells resembling stem cells described in the adult mouse hippocampus (Yu et al. 2014). Ki67$^+$ cells were very sparse or undetectable. MCM2$^+$ cells were more abundant but with a great variability in density. We only found one proliferating Nestin$^+$/Ki67$^+$ cells in the adult human dentate gyrus, while MCM2$^+$/Nestin$^+$ vascular wall cells were more numerous. The latter cells likely correspond to the Nestin-expressing pericytes described in the mouse (Alliot et al. 1999). The fate of Nestin$^+$ or Nestin$^-$ proliferating cells remains unknown. The difficulty in detecting proliferating cells expressing stem cell markers might be due to the short cell cycle of such cells or their low numbers. However, the hypothesis that the number of proliferating cells itself is low is supported by previous studies showing the small number of Ki67$^+$ or MCM2$^+$ proliferating cells (Boekhoorn et al. 2006; Lucassen et al. 2010; Boldrini et al. 2009) and newly generated neurons (Boekhoorn et al. 2006) in the adult human hippocampus compared with rodents (Santos et al. 2007; Imayoshi et al. 2008; Knoth et al. 2010; Spalding et al. 2013). A concomitant study that has just been published also concludes that neurogenesis in the dentate gyrus does not continue, or is extremely rare, in adult humans (Sorrells et al. 2018). In humans, 700 new neurons are estimated to be added to each hippocampus daily, corresponding to an annual turnover of 1.75%, with a modest decline during aging (Spalding et al. 2013). Using proton nuclear magnetic resonance spectroscopy, Manganas et al. (2007) have previously shown that detection of a metabolic biomarker of neural stem/progenitor cells dramatically decreases in the hippocampus of adult individuals (30–35 years) when compared with preadolescent individuals (8–10 years) and adolescent (14–16 years), indicating a major reduction in neural stem/progenitor cell activity during post-adolescent age. We also detected a few small cells expressing DCX, a reliable marker of newborn neurons and neurogenesis during development, especially in combination with TUJ1, but human adult DCX$^+$ cells and their functional properties remain to be characterized *in vivo*.

Our previous study on the human hippocampus suggested that the fimbria could generate other subtypes of neurons than Cajal–Retzius cells during fetal development (Cipriani et al. 2016, 2017). Our present data suggest that fimbrial progenitor cells might form a pool of resting stem cells during the perinatal period and be conserved throughout life. Further studies are necessary to elucidate whether these cells are actually neural stem/progenitor cells and whether they participate in adult granulogenesis or provide neurons to other areas of the brain.

## Neurogenic potential of the dentate gyrus of AD patients

The distribution and morphology of GFAPδ$^+$ and Nestin$^+$ cells in the AD hippocampus are overall similar to those of controls, including the presence of bipolar/unipolar Nestin$^+$ cells resembling stem cells. However, it appeared that close contacts between Nestin$^+$ and/or GFAPδ$^+$ cells and vessels were less obvious compared with control cases. Nevertheless, we could

only perform a semi-quantitative analysis due to the small number of cases, the high variability of labeling within each group and the difference between the two groups in terms of average age. Nestin$^+$ cells have not been detected in patients at Braak stages 3–6 with one of the two anti-Nestin antibodies used in the present study (Kamphuis et al. 2014). In the present study, GFAPδ$^+$ cells were more abundant than Nestin$^+$ cells in the SGZ/hilus of AD donors, in addition to displaying a variable degree of GFAPδ/Nestin and GFAP/Nestin colabeling. GFAPδ$^+$ cells have also been reported by two other studies in AD patients (Roelofs et al. 2005; Kamphuis et al. 2014). Increased GFAPδ transcript levels, but not increased GFAPδ immunoreactivity, have been detected in the hippocampal formation of AD donors (Kamphuis et al. 2014). GFAPδ$^+$ cells predominate in the dentate gyrus compared with the pyramidal layer (Roelofs et al. 2005; Kamphuis et al. 2014) and are not increased in plaque-associated astrocytes in the dentate gyrus (Kamphuis et al. 2014).

Taken together, these data indicate a higher density of GFAPδ$^+$ cells in the dentate gyrus of adult (controls and AD) compared with the fetal and infant hippocampus, and the persistence of Nestin$^+$ and GFAPδ$^+$ cells with putative stem cell properties in the AD hippocampus. However, the functional significance of Nestin or GFAPδ expression remains to be established. Astrogliosis is known to be present in presenile and AD patients (Boekhoorn et al. 2006). Astrocyte activation is characterized by the hypertrophy of cellular processes, upregulation of GFAP, and re-expression of Nestin (Wilhelmsson et al. 2004). Nestin may be expressed in reactive astrocytes and reflects regenerative potential (e.g., in ependymal granulations in this series of patients) in various CNS cell types, but this needs to be further investigated. The rate of proliferation remained very low, comparable to those reported in control patients and we did not find evidence of increased neurogenesis, confirming previous studies in presenile AD patients (Boekhoorn 2006).

The present findings and our previous studies widely characterize the distribution and neurogenic potential of neural stem//progenitor cells in the human hippocampal formation, and provide a reliable framework to better understand the mechanisms of human hippocampal neurogenesis. Specifically, we show the presence of morphologically, topographically, antigenically, and chronologically different subpopulations of stem/progenitor cells during development and aging, including in AD patients. Although the hippocampal SVZ might be a putative neurogenic niche in adult humans, neurogenesis is markedly reduced beyond the perinatal period. In addition, we found no obvious evidence of neurogenic potential in neural stem/progenitor cells in the dentate gyrus beyond 5 years, and few DCX$^+$ neurons were present in adults. Further studies are necessary to investigate the molecular and functional properties of the diverse subsets of neural stem/progenitor cells present in the human hippocampus.

## Supplementary Material

Supplementary material is available at *Cerebral Cortex* online.

## Funding

This work was supported by European Commission FP7-HEALTH-2011-2.2.2-2/Develage (EA, GGK, HA, IF), the Inserm (PG), and Paris Diderot University (PG).

## Notes

We are grateful to Patrice Castagnet, Katia Dossou, and Nathalie Guatto for their technical assistance. *Conflict of interest:* The authors declare that they have no conflict of interest.

## References

Adle-Biassette H, Grassi J, Verney C, Walker F, Choudat L, Hénin D. 2007. Controls in immunohistochemistry. Ann Pathol. 27:16–26.

Alliot F, Rutin J, Leenen PJ, Pessac B. 1999. Pericytes and periendothelial cells of brain parenchyma vessels co-express aminopeptidase N, aminopeptidase A, and nestin. J Neurosci Res. 58:367–378.

Altman J, Bayer SA. 1990a. Mosaic organization of the hippocampal neuroepithelium and the multiple germinal sources of dentate granule cells. J Comp Neurol. 301:325–342.

Altman J, Bayer SA. 1990b. Migration and distribution of two populations of hippocampal granule cell precursors during the perinatal and postnatal periods. J Comp Neurol. 301: 365–381.

Altman J, Bayer SA. 1990c. Prolonged sojourn of developing pyramidal cells in the intermediate zone of the hippocampus and their settling in the stratum pyramidale. J Comp Neurol. 301:343–364.

Bayatti N, Sarma S, Shaw C, Eyre JA, Vouyiouklis DA, Lindsay S, Clowry GJ. 2008. Progressive loss of PAX6, TBR2, NEUROD and TBR1 mRNA gradients correlates with translocation of EMX2 to the cortical plate during human cortical development. Eur J Neurosci. 28:1449–1456.

Bedogni F, Hodge RD, Elsen GE, Nelson BR, Daza RAM, Beyer RP, Bammler TK, Rubenstein JL, Hevner RF. 2010. Tbr1 regulates regional and laminar identity of postmitotic neurons in developing neocortex. Proc. Natl Acad Sci USA. 107:13129–13134.

Berg DA, Yoon KJ, Will B, Xiao AY, Kim NS, Christian KM, Song H, Ming G. 2015. Tbr2-expressing intermediate progenitor cells in the adult mouse hippocampus are unipotent neuronal precursors with limited amplification capacity under homeostasis. Front Biol. 10:262–271.

Betizeau M, Cortay V, Patti D, Pfister S, Gautier E, Bellemin-Ménard A, Afanassieff M, Huissoud C, Douglas RJ, Kennedy H, et al. 2013. Precursor diversity and complexity of lineage relationships in the outer subventricular zone of the primate. Neuron. 80:442–457.

Boekhoorn K, Joels M, Lucassen PJ. 2006. Increased proliferation reflects glial and vascular-associated changes, but not neurogenesis in the presenile Alzheimer hippocampus. Neurobiol Dis. 24(1):1–14.

Boldrini M, Underwood MD, Hen R, Rosoklija GB, Dwork AJ, John Mann J, Arango V. 2009. Antidepressants increase neural progenitor cells in the human hippocampus. Neuropsychopharmacology. 34:2376–2389.

Braak H, Alafuzoff I, Arzberger T, Kretzschmar H, Tredici K. 2006. Staging of Alzheimer disease-associated neurofibrillary pathology using paraffin sections and immunocytochemistry. Acta Neuropathol. 112:389–404.

Braak H, Braak E. 1991. Neuropathological stageing of Alzheimer-related changes. Acta Neuropathol. 82:239–259.

Braak E, Braak H. 1995. Staging of Alzheimer's disease-related neurofibrillary changes. Neurobiol Aging. 16:271–278.

Britanova O, Akopov S, Lukyanov S, Gruss P, Tarabykin V. 2005. Novel transcription factor Satb2 interacts with matrix attachment region DNA elements in a tissue-specific manner and demonstrates cell-type-dependent expression in the developing mouse CNS. Eur J Neurosci. 21:658–668.

Brown J, Cooper-Kuhn CM, Kempermann G, Van Praag H, Winkler J, Gage FH, Kuhn HG. 2003. Enriched environment and physical activity stimulate hippocampal but not olfactory bulb neurogenesis. Eur J Neurosci. 17:2042–2046.

Bystron I, Blakemore C, Rakic P. 2008. Development of the human cerebral cortex: Boulder Committee revisited. Nat Rev Neurosci. 9:110–122.

Cipriani S, Journiac N, Nardelli J, Verney C, Delezoide A-L, Guimiot F, Gressens P, Adle-Biassette H. 2017. Dynamic expression patterns of progenitor and neuron layer markers in the developing human dentate gyrus and fimbria. Cereb Cortex. 27:358–372.

Cipriani S, Nardelli J, Verney C, Delezoide AL, Guimiot F, Gressens P, Adle-Biassette H. 2016. Dynamic expression patterns of progenitor and pyramidal neuron layer markers in the developing human hippocampus. Cereb Cortex. 26: 1255–1271.

Crespel A, Rigau V, Coubes P, Rousset MC, De Bock F, Okano H, Baldy-Moulinier M, Bockaert J, Lerner-Natoli M. 2005. Increased number of neural progenitors in human temporal lobe epilepsy. Neurobiol Dis. 19:436–450.

Dahlstrand J, Lardelli M, Lendahl U. 1995. Nestin messenger-RNA expression correlates with the central-nervous-system progenitor-cell state in many, but not all, regions of developing central-nervous-system. Dev Brain Res. 84: 109–129.

Darsalia V, Heldmann U, Lindvall O, Kokaia Z. 2005. Stroke-induced neurogenesis in aged brain. Stroke. 36:1790–1795.

Decarolis NA, Mechanic M, Petrik D, Carlton A, Ables JL, Malhotra S, Bachoo R, Götz M, Lagace DC, Eisch AJ. 2013. *In vivo* contribution of Nestin- and GLAST-lineage cells to adult hippocampal neurogenesis. Hippocampus. 23:708–719.

Denis-Donini S, Dellarole A, Crociara P, Francese MT, Bortolotto V, Quadrato G, Canonico PL, Orsetti M, Ghi P, Memo M, et al. 2008. Impaired adult neurogenesis associated with short-term memory defects in NF-κB p50-deficient mice. J Neurosci. 28:3911–3919.

Dranovsky A, Picchini AM, Moadel T, Sisti AC, Kimura S, Leonardo ED, Hen R. 2012. Experience dictates stem cell fate in the adult hippocampus. Neuron. 70:908–923.

Eckenhoff MF, Rakic P. 1984. Radial organization of the hippocampal dentate gyrus: a Golgi, ultrastructural, and immunocytochemical analysis in the developing rhesus monkey. J Comp Neurol. 223:1–21.

Encinas JM, Michurina TV, Peunova N, Park J-HH, Tordo J, Peterson DA, Fishell G, Koulakov A, Enikolopov G. 2011. Division-coupled astrocytic differenciation and age-related depletion of neural stem cells in the adult hippocampus. Cell Stem Cell. 8:566–579.

Englund C. 2005. Pax6, Tbr2, and Tbr1 are expressed sequentially by radial glia, intermediate progenitor cells, and postmitotic neurons in developing neocortex. J Neurosci. 25: 247–251.

Eriksson PS, Perfilieva E, Björk-Eriksson T, Alborn AM, Nordborg C, Peterson DA, Gage FH. 1998. Neurogenesis in the adult human hippocampus. Nat Med. 4:1313–1317.

Feng R, Rampon C, Tang YP, Shrom D, Jin J, Kyin M, Sopher B, Miller MW, Ware CB, Martin GM, et al. 2001. Deficient neurogenesis in forebrain-specific presenilin-1 knockout mice is associated with reduced clearance of hippocampal memory traces. Neuron. 32:911–926.

Francis F, Koulakoff A, Boucher D, Chafey P, Schaar B, Vinet MC, Friocourt G, McDonnell N, Reiner O, Kahn A, et al. 1999. Doublecortin is a developmentally regulated, microtubule-associated protein expressed in migrating and differentiating neurons. Neuron. 23:247–256.

Fuchs E. 1998. A structural scaffolding of intermediate filaments in health and disease. Science. 279:514–519.

Gerdes J, Li L, Schlueter C, Duchrow M, Wohlenberg C, Gerlach C, Stahmer I, Kloth S, Brandt E, Flad HD. 1991. Immunobiochemical and molecular biologic characterization of the cell proliferation-associated nuclear antigen that is defined by monoclonal antibody Ki-67. Am J Pathol. 138: 867–873.

Gleeson JG, Peter TL, Flanagan LA, Walsh CA. 1999. Doublecortin is a microtubule-associated protein and is expressed widely by migrating neurons. Neuron. 23:257–271.

Götz M, Stoykova A, Gruss P. 1998. Pax6 controls radial glia differentiation in the cerebral cortex. Neuron. 21: 1031–1044.

Han W, Kwan KY, Shim S, Lam MMS, Shin Y, Xu X, Xu X, Zhu Y, Li M, Sestan N. 2011. TBR1 directly represses Fezf2 to control the laminar origin and development of the corticospinal tract. Proc Natl Acad Sci USA. 108:3041–3046.

Hansen DV, Lui JH, Parker PRL, Kriegstein AR. 2010. Neurogenic radial glia in the outer subventricular zone of human neocortex. Nature. 464:554–561.

Hevner RF, Hodge RD, Daza RAM, Englund C. 2006. Transcription factors in glutamatergic neurogenesis: conserved programs in neocortex, cerebellum, and adult hippocampus. Neurosci Res. 55:223–233.

Hodge RD, Garcia AJ, Elsen GE, Nelson BR, Mussar KE, Reiner SL, Xu X, Zhu Y, Li M, Sestan N. 2013. Tbr2 expression in cajal-retzius cells and intermediate neuronal progenitors is required for morphogenesis of the dentate gyrus. J Neurosci. 33:4165–4180.

Hodge RD, Nelson BR, Kahoud RJ, Yang R, Mussar KE, Reiner SL, Hevner RF. 2012. Tbr2 is essential for hippocampal lineage progression from neural stem cells to intermediate progenitors and neurons. J Neurosci. 32:6275–6287.

Holley JE, Gveric D, Newcombe J, Cuzner ML, Gutowski NJ. 2003. Astrocyte characterization in the multiple sclerosis glial scar. Neuropathol Appl Neurobiol. 29:434–444.

Humphrey T. 1967. The development of the human hippocampal fissure. J Anat. 101:655–676.

Höglinger GU, Rizk P, Muriel MP, Duyckaerts C, Oertel WH, Caille I, Hirsch EC. 2004. Dopamine depletion impairs precursor cell proliferation in Parkinson disease. Nat Neurosci. 7:726–735.

Ibi D, Takuma K, Koike H, Mizoguchi H, Tsuritani K, Kuwahara Y, Kamei H, Nagai T, Yoneda Y, Nabeshima T, et al. 2008. Social isolation rearing-induced impairment of the hippocampal neurogenesis is associated with deficits in spatial memory and emotion-related behaviors in juvenile mice. J Neurochem. 105:921–932.

Imayoshi I, Sakamoto M, Ohtsuka T, Takao K, Miyakawa T, Yamaguchi M, Mori K, Ikeda T, Itohara S, Kageyama R. 2008. Roles of continuous neurogenesis in the structural and functional integrity of the adult forebrain. Nat Neurosci. 11: 1153–1161.

Jin K, Peel AL, Mao XO, Xie L, Cottrell BA, Henshall DC, Greenberg DA. 2004. Increased hippocampal neurogenesis in Alzheimer's disease. Proc Natl Acad Sci USA. 101:343–347.

Kamei Y, Inagaki N, Nishizawa M, Tsutsumi O, Taketani Y, Inagaki M. 1998. Visualization of mitotic radial glial lineage cells in the developing rat brain by Cdc2 kinase-phosphorylated vimentin. Glia. 23:191–199.

Kamphuis W, Middeldorp J, Kooijman L, Sluijs JA, Kooi EJ, Moeton M, Freriks M, Mizee MR, Hol EM. 2014. Glial fibrillary acidic protein isoform expression in plaque related astrogliosis in Alzheimer's disease. Neurobiol Aging. 35: 492–510.

Kempermann G, Gast D, Gage FH. 2002. Neuroplasticity in old age: sustained fivefold induction of hippocampal neurogenesis by long-term environmental enrichment. Ann Neurol. 52:135–143.

Kempermann G, Kuhn HG, Gage FH. 1997. More hippocampal neurons in adult mice living in an enriched environment. Nature. 386:493–495.

Knoth R, Singec I, Ditter M, Pantazis G, Capetian P, Meyer RP, Horvat V, Volk B, Kempermann G. 2010. Murine features of neurogenesis in the human hippocampus across the lifespan from 0 to 100 years. PLoS One. 5:e8809.

Lavado A, Lagutin OV, Chow LML, Baker SJ, Oliver G. 2010. Prox1 Is required for granule cell maturation and intermediate progenitor maintenance during brain neurogenesis. PLoS Biol. 8:43–44.

Lee J, Seroogy KB, Mattson MP. 2002. Dietary restriction enhances neurotrophin expression and neurogenesis in the hippocampus of adult mice. J Neurochem. 80:539–547.

Leid M, Ishmael JE, Avram D, Shepherd D, Fraulob V, Dollé P. 2004. CTIP1 and CTIP2 are differentially expressed during mouse embryogenesis. Gene Expr Patterns. 4:733–739.

Lendahl U, Zimmerman LB, McKay RD. 1990. CNS stem cells express a new class of intermediate filament protein. Cell. 60:585–595.

Leonard BW, Mastroeni D, Grover A, Liu Q, Yang K, Gao M, Wu J, Pootrakul D, van den Berge SA, Hol EM, et al. 2009. Subventricular zone neural progenitors from rapid brain autopsies of elderly subjects with and without neurodegenerative disease. J Comp Neurol. 515:269–294.

Levitt P, Cooper ML, Rakic P. 1981. Coexistence of neuronal and glial precursor cells in the cerebral ventricular zone of the fetal monkey: an ultrastructural immunoperoxidase analysis. J Neurosci. 1:27–39.

Li F, Zhang YY, Jing XM, Yan CH, Shen XM. 2010. Memory impairment in early sensorimotor deprived rats is associated with suppressed hippocampal neurogenesis and altered CREB signaling. Behav Brain Res. 207:458–465.

Liu J, Reeves C, Jacques T, McEvoy A, Miserocchi A, Thompson P, Sisodiya S, Thom M. 2018. Nestin-expressing cell types in the temporal lobe and hippocampus: Morphology, differentiation, and proliferative capacity. Glia. 66:62–77.

Lucassen PJ, Stumpel MW, Wang Q, Aronica E. 2010. Decreased numbers of progenitor cells but no response to antidepressant drugs in the hippocampus of elderly depressed patients. Neuropharmacology. 58:940–949.

Ma Q-H, Futagawa T, Yang W-L, Jiang X-D, Zeng L, Takeda Y, Xu RX, Bagnard D, Schachner M, Furley AJ, et al. 2008. A TAG1-APP signalling pathway through Fe65 negatively modulates neurogenesis. Nat Cell Biol. 10:283–294.

Mamber C, Kamphuis W, Haring NL, Peprah N, Middeldorp J, Hol EM. 2012. GFAPδ expression in glia of the developmental and adolescent mouse brain. PLoS One. 7:1–15.

Manganas LN, Zhang X, Li Y, Hazel RD, Smith SD, Wagshul ME, Henn F, Benveniste H, Djuric PM, Enikolopov G, et al. 2007. Magnetic resonance spectroscopy identifies neural progenitor cells in the live human brain. Science. 318:980–985.

Michalczyk K, Ziman M. 2005. Nestin structure and predicted function in cellular cytoskeletal organisation. Histol Histopathol. 20:665–671.

Middeldorp J, Boer K, Sluijs JA, De Filippis L, Encha-Razavi F, Vescovi AL, Swaab DF, Aronica E, Hol EM. 2010. GFAPδ in radial glia and subventricular zone progenitors in the developing human cortex. Development. 137:313–321.

Mignone JL, Kukekov V, Chiang A-S, Steindler D, Enikolopov G. 2004. Neural stem and progenitor cells in Nestin-GFP transgenic mice. J Comp Neurol. 469:311–324.

Monje ML. 2003. Inflammatory blockade restores adult hippocampal neurogenesis. Science. 302:1760–1765.

Morshead CM, Reynolds BA, Craig CG, McBurney MW, Staines WA, Morassutti D, Weiss S, van der Kooy D. 1994. Neural stem cells in the adult mammalian forebrain: a relatively quiescent subpopulation of subependymal cells. Neuron. 13: 1071–1082.

Nielsen AL, Holm IE, Johansen M, Bonven B, Jorgensen P, Jorgensen AL. 2002. A new splice variant of glial fibrillary acidic protein, GFAP.epsilon., interacts with the presenilin proteins. J Biol Chem. 277:29983–29991.

Nieto M, Monuki ES, Tang H, Imitola J, Haubst N, Khoury SJ, Cunningham J, Gotz M, Walsh CA. 2004. Expression of Cux-1 and Cux-2 in the subventricular zone and upper layers II–IV of the cerebral cortex. J Comp Neurol. 479:168–180.

Palmer TD, Willhoite AR, Gage FH. 2000. Vascular niche for adult hippocampal neurogenesis. J Comp Neurol. 425: 479–494.

Quinn JC, Molinek M, Martynoga BS, Zaki PA, Faedo A, Bulfone A, Hevner RF, West JD, Price DJ. 2007. Pax6 controls cerebral cortical cell number by regulating exit from the cell cycle and specifies cortical cell identity by a cell autonomous mechanism. Dev Biol. 302:50–65.

Reif A, Fritzen S, Finger M, Strobel A, Lauer M, Schmitt A, Lesch KP. 2006. Neural stem cell proliferation is decreased in schizophrenia, but not in depression. Mol.Psychiatry.. 11: 514–522.

Roelofs RF, Fischer DF, Houtman SH, Sluijs JA, Van Haren W, Van Leeuwen FW, Hol EM. 2005. Adult human subventricular, subgranular, and subpial zones contain astrocytes with a specialized intermediate filament cytoskeleton. Glia. 52: 289–300.

Sanai N, Nguyen T, Ihrie RA, Mirzadeh Z, Tsai HH, Wong M, Gupta N, Berger MS, Huang E, Garcia-Verdugo JM, et al. 2011. Corridors of migrating neurons in the human brain and their decline during infancy. Nature. 478:382–386.

Sanai N, Tramontin AD, Quiñones-Hinojosa A, Barbaro NM, Gupta N, Kunwar S, Lawton MT, McDermott MW, Parsa AT, Manuel-García Verdugo J, et al. 2004. Unique astrocyte ribbon in adult human brain contains neural stem cells but lacks chain migration. Nature. 427:740–744.

Santos GM, Southon JR, Griffin S, Beaupre SR, Druffel ERM. 2007. Ultra small-mass AMS 14C sample preparation and analyses at KCCAMS/UCI Facility. Nucl Instrum Methods Phys Res B Beam Interact Mater Atoms. 259:293–302.

Scott BW, Wojtowicz JM, Burnham WM. 2000. Neurogenesis in the dentate gyrus of the rat following electroconvulsive shock seizures. Exp Neurol. 165:231–236.

Shen Q. 2004. Endothelial cells stimulate self-renewal and expand neurogenesis of neural stem cells. Science. 304: 1338–1340.

Smith PD, McLean KJ, Murphy MA, Turnley AM, Cook MJ. 2006. Functional dentate gyrus neurogenesis in a rapid kindling seizure model. Eur J Neurosci. 24:3195–3203.

Sorrells SF, Paredes MF, Cebrian-Silla A, Sandoval K, Qi D, Kelley KW, James D, Mayer S, Chang J, Auguste KI, et al. 2018. Human hippocampal neurogenesis drops sharply in children to undetectable levels in adults. Nature. 555: 377–381. doi: 10.1038/nature25975.

Spalding KL, Bergmann O, Alkass K, Bernard S, Salehpour M, Huttner HB, Boström E, Westerlund I, Vial C, Buchholz BA, et al. 2013. Dynamics of hippocampal neurogenesis in adult humans. Cell. 153:1219–1227.

Szemes M, Gyorgy A, Paweletz C, Dobi A, Agoston DV. 2006. Isolation and characterization of SATB2, a novel AT-rich DNA binding protein expressed in development- and cell-specific manner in the rat brain. Neurochem Res. 31:237–246.

Tavazoie M, Van der Veken L, Silva-Vargas V, Louissaint M, Colonna L, Zaidi B, Garcia-Verdugo JM, Doetsch F. 2008. A specialized vascular niche for adult neural stem cells. Cell Stem Cell. 3:279–288.

van den Berge SA, Middeldorp J, Eleana Zhang C, Curtis MA, Leonard BW, Mastroeni D, Voorn P, van de Berg WD, Huitinga I, Hol EM, et al. 2010. Longterm quiescent cells in the aged human subventricular neurogenic system specifically express GFAP-δ. Aging Cell. 9:313–326.

van den Berge SA, Van Strien ME, Korecka JA, Dijkstra AA, Sluijs JA, Kooijman L, Eggers R, De Filippis L, Vescovi AL, Verhaagen J, et al. 2011. The proliferative capacity of the subventricular zone is maintained in the parkinsonian brain. Brain. 134:3249–3263.

van Praag H, Christie BR, Sejnowski TJ, Gage FH. 1999. Running enhances neurogenesis, learning, and long-term potentiation in mice. Proc Natl Acad Sci U S A. 96: 13427–13431.

van Praag H, Kempermann G, Gage FH. 1999. Running increases cell proliferation and neurogenesis in the adult mouse dentate gyrus [Internet]. Nat Neurosci. 2:266–270.

Wen PH, Hof PR, Chen X, Gluck K, Austin G, Younkin SG, Younkin LJ, DeGasperi R, Gama Sosa MA, Robakis NK, et al. 2004. The presenilin-1 familial Alzheimer disease mutant P117L impairs neurogenesis in the hippocampus of adult mice. Exp Neurol. 188:224–237.

Wilhelmsson U, Li L, Pekna M, Berthold CH, Blom S, Eliasson C, Renner O, Bushong E, Ellisman M, Morgan TE, et al. 2004. Absence of glial fibrillary acidic protein and vimentin prevents hypertrophy of astrocytic processes and improves post-traumatic regeneration. J Neurosci. 24:5016–5021.

Winocur G, Wojtowicz JM, Sekeres M, Snyder JS, Wang S. 2006. Inhibition of neurogenesis interferes with hippocampus-dependent memory function. Hippocampus. 16:296–304.

Yu DX, Marchetto MC, Gage FH. 2014. How to make a hippocampal dentate gyrus granule neuron. Development. 141: 2366–2375.

Zecevic N, Milosevic A, Rakic S, Marin-Padilla M. 1999. Early development and composition of the human primordial plexiform layer. J Comp Neurol. 412:241–254.